Lytic bacteriophages facilitate antibiotic sensitization of *Enterococcus faecium*

Gregory S. Canfield,[a,b] Anushila Chatterjee,[b] Mihnea R. Mangalea,[b] Emma K. Sheriff,[b] Micah Keidan,[b] Sara W. McBride,[b,*] Bruce D. McCollister,[a] and Breck A. Duerkop[b,#]

[a]Division of Infectious Diseases, University of Colorado School of Medicine, Aurora, Colorado, USA

[b]Department of Immunology and Microbiology, University of Colorado School of Medicine, Aurora, Colorado, USA

[#]Correspondence: Breck A. Duerkop breck.duerkop@cuanschutz.edu

[*]Current address: Salk Institute, La Jolla, California, USA

Running Title: Phages enhance antibiotic susceptibility of *E. faecium*

Key words: bacteriophages, *Enterococcus*, antibiotic resistance, phage–bacteria interactions, phage resistance, cephalosporin, beta-lactams

Abstract

Enterococcus faecium, a commensal of the human intestine, has emerged as a hospital-adapted, multi-drug resistant (MDR) pathogen. Bacteriophages (phages), natural predators of bacteria, have regained attention as therapeutics to stem the rise of MDR bacteria. Despite their potential to curtail MDR *E. faecium* infections, the molecular events governing *E. faecium*-phage interactions remain largely unknown. Such interactions are important to delineate because phage selective pressure imposed on *E. faecium* will undoubtedly result in phage resistance phenotypes that could threaten the efficacy of phage therapy. In an effort to understand the emergence of phage resistance in *E. faecium*, three newly isolated lytic phages were used to demonstrate that *E. faecium* phage resistance is conferred through an array of cell wall-associated molecules, including secreted antigen A (SagA), enterococcal polysaccharide antigen (Epa), wall teichoic acids, capsule, and an arginine-arginine-aspartate (RDD) protein of unknown function. We find that capsule and Epa are important for robust phage adsorption and that phage resistance mutations in *sagA*, *epaR*, and *epaX* enhance *E. faecium* susceptibility to ceftriaxone, an antibiotic normally ineffective due to its low affinity for enterococcal penicillin binding proteins. Consistent with these findings, we provide evidence that phages potently synergize with cell wall (ceftriaxone and ampicillin) and membrane-acting (daptomycin) antimicrobials to slow or completely inhibit the growth of *E. faecium*. Our work demonstrates that the evolution of phage resistance comes with fitness defects resulting in drug sensitization and that lytic phages could potentially serve as antimicrobial adjuvants in treating *E. faecium* infections.

55 **Introduction.**

56 Enterococci are intestinal commensal bacteria and important opportunistic human pathogens
57 (1). Of the two most clinically relevant enterococcal species, *Enterococcus faecalis* and *Enterococcus*
58 *faecium*, the emergence of multidrug resistance is observed most commonly with *E. faecium* (2).
59 Considering that effective antibiotics with activity against multidrug-resistant (MDR) *E. faecium* are
60 limited, clinicians are often forced to use antibiotic combination therapy to treat these infections (3).
61 Although this approach can be life-saving, these regimens increase the risk of patient adverse drug
62 events, drug-drug interactions, dysbiosis, and may fail to cure the infection (4). Rising from desperate
63 treatment dilemmas like these are several examples of the successful use of phage therapy to treat
64 MDR bacterial infections in humans (5-8). These success-stories have motivated renewed interest in
65 the use of phage therapy for treatment of bacterial infections. Despite this motivation, relatively little is
66 understood about the bacterial receptors exploited by phages to infect their bacterial hosts and the
67 counter-measures employed by bacteria to avoid phage infection. We believe that understanding the
68 molecular events that lead to phage resistance in MDR bacteria may help mitigate the threat of phage
69 therapy failure.

70 Recently, our group and others have begun to elucidate the molecular mechanisms that enable
71 successful phage infection of enterococci and the bulk of these studies were performed for *E. faecalis*
72 and its interactions with tailed dsDNA phages. (9-15). The molecular mechanisms enabling phage
73 infection in *E. faecium* are not well studied. Our knowledge of potential *E. faecium* phage receptors
74 comes from an *in vitro* study where phage and *E. faecium* co-existence was challenged through
75 multiple passages in laboratory media (12). Whole genome sequencing of phage resistant survivors
76 showed mutations in the capsule tyrosine kinase *ywqD2* (equivalent to *wze*), RNA polymerase β-
77 subunit (*rpoC*), several predicted hydrolases, and a cell wall precursor enzyme. It was proposed that
78 these mutations conferred phage resistance, though direct genetic testing of this hypothesis was not
79 performed. Tandem-duplications in a putative phage tail fiber gene (EFV12PHI1_98) supported
80 evolution of phages that overcame adaptive changes that resulted in phage resistance of *E. faecium*
81 (12).

82 In this work, we expand on our understanding of phage-enterococcal interactions by identifying
83 genes important for lytic phage infection of *E. faecium.* We have isolated three previously
84 uncharacterized *E. faecium*-specific phages and show that each belong to the *Siphoviridae* morphotype
85 of the *Caudovirales* and resemble previously described lytic enterococcal phages (9-11, 14). Protein
86 coding sequence comparison to other enterococcal phages reveals that one phage belongs to a novel
87 enterococcal phage orthocluster and the remaining two phages belong to previously described
88 enterococcal phage orthoclusters (16). To identify the molecular determinants of *E. faecium* phage
89 infection, we used these three phages to generate a collection of *E. faecium* phage resistant mutants.
90 Phage resistance mutations mapped to genes encoding the cell wall hydrolase secreted antigen A
91 (*sagA*), putative teichoic acid precursors of the enterococcal polysaccharide antigen (*epa*), capsule
92 biosynthesis enzymes, and an arginine-aspartate-aspartate (RDD) protein. Capsule and putative
93 teichoic acid biosynthesis genes, but not SagA, were shown to mediate phage adsorption. Considering
94 that all of the genes identified are involved in cell wall biochemistry and/or architecture, we determined
95 if these phage resistance mutations result in fitness tradeoffs that lead to altered antimicrobial
96 susceptibility. Phage resistant strains harboring mutations in *sagA*, *epaX*, and *epaR* showed enhanced
97 susceptibility to cell wall and/or membrane-acting antibiotics, including ceftriaxone, ampicillin, and
98 daptomycin. We discovered that combining phages with cell wall or membrane-acting antimicrobials
99 acts synergistically to kill *E. faecium*. These findings suggest lytic phages might be leveraged as
100 antibiotic adjuvants to offset the emergence of multi-drug resistant strains of *E. faecium* in hospitalized
101 patients.
102
103 **Results.**
104 **Genome sequence analysis and morphology of novel lytic *E. faecium* bacteriophages.** *E.*
105 *faecium* phages 9181, 9183 and 9184 were isolated from raw sewage by plaque assay using *E.*
106 *faecium* clade B strains Com12 and 1,141,733 (17). Evaluation of phage morphology by TEM revealed
107 that all three phages were non-contractile tailed phages characteristic of the *Siphoviridae* morphotype
108 (Fig. 1) (18). DNA sequence analysis demonstrated that the phage 9181, 9183 and 9184 genomes are

109 71,854bp, 86,301bp, and 44,601bp in length, respectively (Fig. 1). The genomes of phages 9181 and
110 9183 were assembled into single contigs. The phage 9184 genome assembled into two contigs, with a
111 53-bp sequencing gap located near the 5' end of a predicted BppU-family phage baseplate upper
112 protein. In total, 123, 128, and 73 open reading frames (ORFs) were identified for phages 9181, 9183
113 and 9184, respectively (Table S1). Genome modularity based on predicted gene function was
114 observed for each phage genome, however, for phage 9181 the lysin and holin genes are located at
115 the 5' and 3' termini of the genome (Fig. 1). Functional classifications, consisting of replication or
116 biosynthesis, DNA packaging, phage particle morphogenesis, nucleic acid restriction and modification,
117 host cell lysis, sensory function, sugar transferase and potential β-lactamase, could be predicted for
118 approximately 30%, 47%, and 48% of the phage 9181, 9183, and 9184 ORFs, respectively (Table S1).
119 The remaining genes were predicted to be hypothetical genes or genes containing domains of unknown
120 function. The absence of genes encoding Cro repressor-family proteins, toxin-antitoxin genes, and
121 putative integrase genes (except for phage 9183, discussed below) indicates that that phages 9181,
122 9183, and 9184 are obligately lytic.
123
124 **Comparative genome analysis places phages 9181, 9183, and 9184 in distinct orthoclusters.**
125 Comparative genome analysis of phages 9181, 9183 and 9184 was performed with all publicly
126 available enterococcal phage genomes using OrthoMCL, an algorithm that identifies clusters of
127 orthologous proteins from at least two phages enabling phylogenetic categorization of phage proteins
128 into "orthoclusters" (16, 19). Of the 10 enterococcal phage orthoclusters originally identified by Bolocan
129 et al. (16), OrthoMCL clustering places phage 9184 into orthocluster I and phage 9183 into orthocluster
130 X (Fig. 2). Phage 9181 forms a new orthocluster that we have named orthocluster XI (Fig. 2). Whole
131 genome alignments of phages 9183 and 9184 to their nearest orthocluster neighbors, VPE25 and VFW
132 for 9183 and vB_EfaS-DELF1 and IME-EFm5 for 9184, revealed conserved protein sequence identity
133 and similar genome organization (Fig. S1A and S1B). Conversely, phage 9181 shared little protein
134 sequence identity and genome organization to its nearest neighbors, phage EFC-1 and phage FL4A,
135 supporting its placement as the sole member of a new orthocluster (Fig. S1C). Higher protein sequence

136 identity and more similar genome organization was observed for phages belonging to the same
137 orthocluster rather than phages belonging to different orthoclusters. Since the publication of Bolocan et
138 al., an additional 45 phage genomes have been made publically available, resulting in the identification
139 of a 12th orthocluster consisting of phages EFA-1 and EFA-2, two recently described phages of
140 unknown morphology (Fig. 2). Consistent with prior observations of orthocluster I phages, a β-
141 lactamase domain-containing protein (ORF35) was found in the genome of phage 9184 (Fig. 1 and
142 Table S1). Similar to phages in orthocluster X, an integrase-family recombinase was found in the
143 genome of phage 9183 (Table S1). However, prior evidence demonstrates that other members of this
144 orthocluster are unable to lysogenize their *E. faecalis* host (11).
145
146 ***E. faecium* phages have broad and narrow tropism for laboratory and clinical *E. faecium***
147 **isolates.** We next sought to determine the host range of each phage against strains of *E. faecium* and
148 *E. faecalis*. To achieve this, a phage susceptibility assay was performed by spotting 10-fold serially-
149 diluted enterococcal cultures on Todd-Hewitt broth (THB) agar embedded with phages 9181, 9183 or
150 9184. A panel of 10 laboratory *E. faecium* isolates and 11 contemporary MDR clinical *E. faecium*
151 isolates were selected for this analysis (Table S4) (17). An *E. faecium* strain was considered phage-
152 susceptible if less than 1 x 10^5 CFU/mL were recovered following phage exposure, representing greater
153 than 4-log of bacterial killing. Phages 9181 and 9183 demonstrated narrow host ranges against
154 laboratory *E. faecium* strains (Fig. 3A). Besides the host strain on which the phage was isolated
155 (Com12 for phage 9181 and 1,141,733 for phage 9183), only *E. faecium* Com15 was susceptible to
156 phage 9181, while no other *E. faecium* laboratory strain tested was susceptible to phage 9183.
157 Contrarily, 60% of the laboratory *E. faecium* strains were susceptible to phage 9184 (Fig. 3A). There
158 was an absence of susceptibility to phage 9181 and 9183, and reduced susceptibility (~36%) to phage
159 9184 for the contemporary MDR clinical *E. faecium* isolates (Fig. 3B). Together these data show that
160 phage 9184 has a broader host range compared to phages 9181 and 9183. Interestingly, *E. faecium*
161 1,231,501 and 1,230,933, the latter of which is multi-drug resistant, lacked susceptibility to phage 9181,
162 9183 and 9184. None of the three phages were capable of infecting any of the 10 clinical *E. faecalis*

163 strains tested (designated UCH12-20 in Table S4), suggesting that these phages are specific for *E.*
164 *faecium*.
165
166 **Phage predation elicits spontaneous and stable phage resistance in *E. faecium*.** To identify *E.*
167 *faecium* genes that are involved in phage infection, we isolated spontaneous phage-resistant *E.*
168 *faecium* strains following exposure to phages 9181, 9183 and 9184. Phage-resistant isolates were
169 identified by plating stationary phase cultures of *E. faecium* Com12 and 1,141,733 on THB agar
170 embedded with phages 9181, 9183, or 9184. Colonies that arose on these plates represented potential
171 phage-resistant colonies. To confirm the stability of the phage-resistant phenotype, a colony was
172 serially passaged daily for 3 days on THB agar before re-streaking again on phage embedded THB
173 agar. The growth of a strain in the presence of phage following serial passage suggested a stable
174 phage-resistant phenotype (Fig. 4A-C). For phages 9181 and 9183 resistant *E. faecium* strains
175 (denoted 81R3-8 and 83R1-8, respectively) we observed bacterial growth in the presence of phages to
176 levels that were similar to bacterial growth in the absence of phages indicating a strong resistance
177 phenotype (Fig. 4A, 4B and Fig. S2A, S2B, S2D, S2E). However, for phage 9184 we observed limited
178 phage resistance in all but one presumed *E. faecium* phage resistant isolate (Fig. 4C and Fig. S2C,
179 S2F) suggesting that robust resistance to phage 9184 may be multifactorial.
180
181 ***E. faecium* phage resistance mutations occur in cell wall biosynthesis and architecture genes**
182 **and a gene encoding a transmembrane protein.** To identify genetic changes conferring a phage
183 resistance phenotype, we performed whole genome DNA sequencing of phage resistant and parental
184 *E. faecium* strains. We observed unique and conserved genome mutations in strains that had
185 developed phage resistance (Fig. 5A-D and Table S2).
186 Five of six mutations identified in phage 9181-resistant strains were detected in *efvg_rs16270*,
187 which in the *E. faecium* Com12 reference genome is annotated as a hypothetical protein and was
188 flanked by a 5' sequencing gap. Closure of this sequencing gap by PCR and amplicon sequencing
189 revealed that *efvg_rs16270* encodes the *E. faecium* secreted antigen A (SagA) protein. Whole genome

190 sequencing showed that all *sagA* mutations localized at or near the peptidoglycan clamp or active site
191 residues of the NlpC_P60 hydrolase domain of SagA, which was recently shown to function as an
192 endopeptidase that cleaves crosslinked Lys-type peptidoglycan fragments (Fig. 5A and Table S2A)
193 (20). To determine the impact of *sagA* mutations on protein structure and function, each single
194 nucleotide polymorphism-associated *sagA* mutant was assessed by Missense 3D analysis (21).
195 BLASTp alignment of SagA from *E. faecium* Com12 and Com15 showed 95% identity along the entire
196 length of the protein and *E. faecium* Com12 and Com15 exhibit identical protein homology in the
197 NlpC_P60 hydrolase domain (Fig. S3), suggesting that SagA should be functionally conserved between
198 these two stains. Therefore, we used the *E. faecium* Com15 NlpC_P60 crystal structure (PDB 6B8C) in
199 Missense 3D to assess the impact of residue changes on the structure and function of NlpC_P60
200 hydrolase in our *sagA* mutant strains (20). Except for one SagA mutant (81R8; G435V), no structural
201 damaging mutations were found. Given that the potential for structural damage in our *sagA* mutants
202 was low, the observation that all mutations occurred in the NlpC_P60 hydrolase domain, and the fact
203 that *sagA* has been shown to be an essential gene in *E. faecium*, we suspect that these *sagA* mutants
204 represent hypomorphs whose expression levels or catalytic activity are reduced (20, 22, 23).
205 Interestingly, hypomorphs have been observed in the *E. faecalis* SagA-like peptidoglycan hydrolase
206 SalB (24). We complemented the *sagA* mutations in phage 9181 resistant strains using a construct
207 previously generated, pAM401-*sagA*, which carries the *sagA* gene and its native promoter from *E.*
208 *faecium* Com15 (22). For all *sagA* mutants, complementation with pAM401-*sagA* restored phage
209 susceptibility (Fig. S4A). This results suggests that non-crosslinked peptidoglycan in *E. faecium*
210 Com12 is essential for phage 9181 infection.
211 One phage 9181-resistant strain (81R7) harbored mutations in capsule tyrosine kinase (*wze*)
212 and topoisomerase III (*topB*) genes and lacked a *sagA* mutation (Table S2A). Similarly, sequencing
213 analysis of all 9184 resistant strains (84R1-6) revealed an assortment of mutations in the capsule
214 biosynthesis locus. Nonsense, insertion and deletion mutations were detected in *wze*, capsule
215 aminotransferase (*efsg_rs08090*), capsule polymerase (*wzy*), and capsule nucleotide sugar
216 dehydrogenase (*efsg_rs08120*) genes (Fig. 5B and Table S2C). Prior co-evolution experiments

217 between the *Myoviridae* phage 1 and *E. faecium* TX1330 revealed a propensity for *wze* mutations
218 within an evolved phage resistant *E. faecium* population (12). Our data is consistent with this
219 observation and suggests that *E. faecium* capsule might serve as a possible receptor and/or adsorption
220 factor for phages 9181 and 9184. Despite the abundance of capsule mutations detected among our
221 mutant strains, complementation of capsule alleles in capsule mutants minimally restored or failed (Fig.
222 S4B-C) to restore phage 9181 and 9184 susceptibility. This result suggests that capsule is not a major
223 receptor mediating phage resistance to phage 9181 (Fig. S4B) and only weakly promotes phage 9184
224 resistance (Fig. S4C). These results emphasize the importance of other non-capsule associated
225 mutations in conferring phage-resistance to phage 9181 (*sagA*) and phage 9184. We attempted to
226 address the non-capsule associated mutation in strain 81R7 (*topB*) and its involvement in phage 9181
227 resistance, however, all attempts to clone *topB* into the expression vector pLZ12A resulted in truncated
228 *topB* inserts following transformation into *Escherichia coli*, suggesting that constitutive expression of *E.*
229 *faecium topB* may be toxic to *E. coli*. Similarly, to address the role of the non-capsule mutation detected
230 in 84R6, which exhibited a robust phage 9184-resistance phenotype, a predicted arginine-aspartate-
231 aspartate gene (*rdd*), this gene was successfully cloned into pLZ12A yet transformation of this
232 construct into *E. faecium* 84R6 was unsuccessful despite repeated attempts. Given the ease with which
233 pLZ12A-*wze* and empty pLZ12A vector were transformed into *E. faecium* 84R6 and our repeated
234 failure to successfully recover transformants harboring pLZ12A-*rdd* suggests that over-expression of
235 *rdd* in *E. faecium* 84R6 may be lethal.
236 Analysis of *E. faecium* phage 9183 resistant strains (83R1-8) identified mutations in *epa* genes,
237 *epaR* and *epaX* (Fig. 5D and Table S2B). Mutation of *epaR* and *epaX* results in *E. faecalis* phage
238 resistance (9, 10, 14) and recently it was determined that the *epaR* and *epaX* genes of *E. faecalis* V583
239 participate in wall teichoic acid biosynthesis (25). Considering that mutation of the *epaX* homologs
240 *epaOX* and *epaOX2* from *E. faecalis* OG1RF conferred phage VPE25-resistance by limiting phage
241 adsorption (10, 11), we suspect that teichoic acids also mediate adsorption of phage 9183 to *E.*
242 *faecium* 1,141,733. We were surprised that we did not find any phage 9183 resistant strains with
243 mutations in PIP_{EF}, given the high protein homology and similar genome organization observed

244 between phages 9183, VPE25 and VFW, the latter two which use PIP_{EF} as a receptor (11) (Fig. 2). To
245 confirm that mutations in the *epa* locus confer phage resistance in *E. faecium*, we pursued a similar
246 complementation strategy as above with the *epaR* and *epaX* mutants identified in the phage 9183-
247 resistant mutants. All phage 9183-resistant mutants complemented with either the *epaR* or *epaX* were
248 restored for phage susceptibility (Fig. S4D). Given the importance of D-alanylation in teichoic acid
249 biosynthesis, we performed complementation with pLZ12A-*dltA* in the *epaX* and *dltA* double mutant
250 (83R7). We observed that only pLZ12A-*epaX*, not pLZ12A-*dltA*, was capable of restoring phage
251 susceptibility in 83R7 (Fig. S4D). Considering that EpaX acts upstream of DltA in the biosynthesis of
252 teichoic acids (25), these data suggest that *dltA* is dispensable during phage infection, lending further
253 support to the notion that the *epa* variable locus involved in teichoic acid biosynthesis is a driver of *E.*
254 *faecium* infection by phage 9183.
255
256 ***E. faecium* phage resistant mutants have phage adsorption defects.** To determine if phage
257 adsorption defects occur due to phage resistance, we sought to quantify phage 9181, 9183, and 9184
258 adsorption to wild type and phage resistant *E.* faecium strains using a phage attachment assay (9, 10,
259 14). For phage 9181 resistant strains, we observed no significant change in adsorption to *sagA* mutant
260 strain 81R5 and a modest change in phage adsorption to the phage resistant strain 81R7 harboring a
261 *wze* and *topB* mutations (Fig. 6A). This result suggests that mutation of *sagA* in *E. faecium* Com12 has
262 little to no effect on phage 9181 adsorption. It is possible that mutation of *wze* contributes to phage
263 binding, however, we cannot rule out the possibility that mutation of *topB* in this mutant background
264 causes transcriptional or translational changes in surface expressed molecules that result in the modest
265 phage 9181 adsorption phenotype (Fig. 6A).
266 Previous work has demonstrated that *epa* mutants exhibit phage adsorption defects in *E.*
267 *faecalis* (9, 10, 13, 14). Since we observed *epa* mutations that conferred phage 9183 resistance, we
268 sought to determine if *epa* mutations might promote a similar phenotype in *E. faecium*. We observed a
269 reduction in phage 9183 adsorption to mutants possessing *epaR* (83R6 and 83R8) and *epaX* (83R4
270 and 83R7) mutations compared with the parental strain (Fig. 6B). Although *epaX* mutants 83R4 and

271 83R7 were noted to also have mutations in *gdh* and *dltA*, respectively, we suspect that EpaX was the
272 driver of this phenotype because of the known role of *epaX* homolog mutations to inhibit phage VPE25
273 adsorption to *E. faecalis* and that EpaX functions upstream of DltA in the biosynthesis of teichoic acid
274 (10, 25). Taken together, these results suggest that mutations in the *epa* locus of *E. faecium* lessen
275 phage 9183 adsorption to the surface of its host strain.
276 To determine if mutations in the capsule locus facilitated phage 9184 adsorption defects, we
277 performed phage 9184 adsorption assays using wild type and phage 9184 resistant mutants. We
278 observed significant deficits in phage adsorption to strains harboring mutations in capsule polymerase
279 (84R1), nucleotide sugar dehydrogenase (84R4), and tyrosine kinase (84R6) in comparison to the
280 parental strain (Fig. 6C). Given that 84R6 also harbors an *rdd* mutation which encodes a putative
281 transmembrane protein, we cannot definitively conclude that the adsorption deficit was related to the
282 capsule tyrosine mutation, as this mutation only manifested as a mild adsorption defect for phage 9181
283 (Fig. 6A). Considering the adsorption defect is greater for the capsule mutants raised against phages
284 9184 compared to the phage 9181 capsule mutant 81R7, it is possible that additional surface
285 associated molecules mediate the attachment of phage 9181 to *E. faecium* cells. Together, these data
286 indicate that *E. faecium* capsule contributes to phage adsorption and may be phage specific.
287
288 ***E. faecium* phage resistance enhances β-lactam and lipopeptide susceptibility.** With renewed
289 interest focused on utilizing lytic phages for the treatment of bacterial infections and the observation
290 that phage resistance can be a fitness tradeoff under antibiotic pressure (26, 27), we sought to
291 determine the impact of *E. faecium* phage resistance on antimicrobial susceptibility. We performed
292 antimicrobial susceptibility screening using E-test strips for the phage 9181, 9183, and 9184 resistant
293 mutants compared to their parental strains to determine if phage resistance altered *E. faecium*
294 antimicrobial susceptibility. For phage 9181 resistant mutants, we observed a 2-5 fold reduction in the
295 minimum inhibitory concentration (MIC) of ampicillin and an 8-32 fold reduction in the MIC of
296 ceftriaxone (Table S3A). Interestingly, the enhancement of ampicillin and ceftriaxone susceptibility
297 correlated with phage 9181 resistant mutants harboring mutations in *sagA*, and not *wze* or *topB*. For

298 phage 9183 resistant mutants, we also observed a 5-8 fold reduction in the MIC of ampicillin and 16-
299 128 fold reduction in the MIC of ceftriaxone (Table S3B). Additionally, we noted a 1.5-3 fold reduction
300 in the MIC of daptomycin, a lipopeptide class antimicrobial, which was not observed for the phage 9181
301 resistant mutants. These results suggest that the acquisition of phage resistance via mutation of *sagA*
302 and *epa* genes in *E. faecium* is a fitness defect that manifests as enhanced β-lactam susceptibility.
303 No phage capsule mutants showed a significant difference in antimicrobial susceptibility to β-
304 lactams or lipopeptides, suggesting that mutations to the *E. faecium* capsule locus and *rdd* avoid the
305 cost of increased antimicrobial susceptibility (Table S3C).
306
307 **Lytic phages synergize with β-lactam and lipopeptide antimicrobials to enhance the killing of *E.***
308 ***faecium*.** Considering the antibiotic fitness cost associated with phage resistance in *E. faecium*, we
309 hypothesized that phages 9181 and 9183 would be capable of synergizing with ampicillin, ceftriaxone,
310 and daptomycin to kill *E. faecium*. To address this question, we performed phage-antibiotic synergy
311 assays where *E. faecium* was grown in the presence of phages alone, sub-inhibitory concentrations of
312 ampicillin, ceftriaxone, or daptomycin alone, or a combination of phage and a sub-inhibitory
313 concentration of antibiotics (Fig. 7A-E). For all three antibiotics, we observed that the combination of
314 phage and sub-inhibitory concentrations of antibiotics were able to inhibit the growth of *E. faecium*
315 better than phage or antibiotic alone. Given the absence of growth inhibition of *E. faecium* in the
316 presence of sub-inhibitory concentrations of antibiotics alone, this result is consistent with a synergistic
317 antimicrobial interaction between phages and antibiotics. Interestingly, the synergy observed between
318 phages 9181 and 9183 and ceftriaxone appeared more potent than the synergy observed between
319 these phages and ampicillin (Fig. 7A-D). A dose-response relationship emerged when ampicillin was
320 combined phages 9181 and 9183 where decreasing concentrations of ampicillin enabled varying
321 degrees of bacterial population recovery (Fig. 7A-B). These data suggest that phages 9181 and 9183
322 could serve as useful adjuvants in combination with β-lactams for the treatment of *E. faecium* infections
323 by restoring the susceptibility to *E. faecium* strains harboring intrinsic β-lactam resistance. We also
324 observed that the combination of phage 9183 and daptomycin slowed the growth of *E. faecium*

325 1,141,733 more than phage 9183 alone or daptomycin alone (Fig. 7E). This suggests that phage 9183
326 also synergizes with daptomycin to inhibit *E. faecium* 1,141,733. These results are consistent with
327 those observed by Morrisette et al. who observed synergy between the *Myoviridae* phage 113 and β-
328 lactam (ampicillin, ertapenem and ceftaroline) and lipopeptide antimicrobials against daptomycin-
329 resistant and tolerant strains of *E. faecium* (28).
330
331 **Discussion.**
332 Considering the treatment pitfalls due to worsening drug resistance in *E. faecium* and other
333 bacterial pathogens, the biomedical community is revisiting the use of phage therapy. Since phage
334 therapy's departure from 20th century Western Medicine, new technologies have emerged that have
335 facilitated fine-scale resolution of phage-bacterial molecular interactions. Despite these advancements,
336 for many bacteria, including *E. faecium*, the molecular factors exploited by phages for infection remain
337 largely understudied (12). We believe that studying the molecular interactions of phages with their *E.*
338 *faecium* hosts will inform rational approaches for future phage therapies against this pathogen.
339 In this work, we describe three novel lytic phages of *E. faecium*. Using protein coding orthology,
340 we show that one of these phages, phage 9181, forms a new orthocluster from the ten previously
341 described enterococcal phage orthoclusters (16). We show that these phages are specific for *E.*
342 *faecium* and exhibit broad and narrow strain tropism. Using whole genome sequencing and
343 comparative genomics, we provide evidence that *sagA*, *epa*, and capsule biosynthesis genes are
344 important for phage infection of *E. faecium*. We were unable to fully assess if the genes *topB* and *rdd*
345 are important in mediating phage 9181 and phage 9184 resistance, respectively. We suspect that these
346 genes aid in phage-*E.faecium* interactions. Consistent with previous observations in *E. faecalis* (9, 10,
347 13, 14), we show that mutations in *epaR* and *epaX* limit phage 9183 adsorption to *E. faecium*. Similarly,
348 we show for the first time that mutations in the capsule locus, which is absent in *E. faecalis* (17), limits
349 phage 9181 and 9184 adsorption to *E. faecium*.
350 Our investigation into fitness tradeoffs associated with *E. faecium* phage resistance revealed
351 enhanced susceptibility to cell wall and membrane-acting antibiotics. We demonstrated that phages

352 9181 and 9183 synergize with cell wall and membrane-targeting antibiotics to more potently inhibit *E.*
353 *faecium*. Importantly, this analysis revealed that phages 9181 and 9183 could sensitize *E. faecium* to
354 ceftriaxone, an antibiotic that normally promotes enterococcal colonization of the intestine due to
355 intrinsic resistance (29). Phage synergy with ceftriaxone is an important discovery as it suggests a
356 strategy to re-sensitize enterococci to a third-generation cephalosporin. Exposure to cell wall-acting
357 agents is recognized as a key event prior to hospital-acquired enterococcal infection in susceptible
358 patients and cephalosporin re-sensitization could have a broad impact on anti-enterococcal therapy (2,
359 30). Cephalosporin activity pressures the native intestinal microbiota altering its ecology and related
360 mucosal immunity, creating a scenario for enterococci to thrive and become dominant members of the
361 microbiota (30-33). In patients with weakened immune systems or made vulnerable from hospital
362 procedures such as surgeries, bone marrow ablative chemotherapy, or pre-existing alcoholic
363 hepatitis/cirrhosis, these ceftriaxone-associated conditions can tip the scale in favor of infection (30-32,
364 34, 35). Even in *E. faecium* strains with ampicillin susceptibility, synergy with ceftriaxone for the
365 treatment of endocarditis was demonstrated to be not absolute, suggesting that current Infectious
366 Disease Society of America guidelines for the treatment of *E. faecium* endocarditis may lead to sub-
367 optimal results (36, 37). Combination therapy with phage and cell wall or membrane-acting
368 antimicrobials may offer a potential solution to circumvent this issue, while avoiding the risk associated
369 with exposing patients to combination β-lactam agents.
370 Previous studies indicate that intrinsic resistance to ceftriaxone is derived from not only a low-
371 affinity penicillin binding protein 5 (Pbp5), but also *pbpA*, *ponA* and *pbpf* genes in *E. faecium* (38-41).
372 However, in *ponA* and *pbpf* mutants a dissociation in penicillin and cephalosporin susceptibility was
373 observed in *E. faecium* whereby these mutants were rendered susceptible to cephalosporins, but unlike
374 a *pbp5* mutant, not ampicillin, (40). Interestingly, PbpA was found to be essential in *E. faecium* and also
375 exhibited low affinity for both ampicillin and ceftriaxone (38). Combining this observation with the
376 enhancement of ampicillin and ceftriaxone susceptibility displayed by *sagA*, *epaR* and *epaX* mutants, it
377 suggests that Pbp5 and PbpA may play a role in conferring β-lactam susceptibility in these phage
378 resistant mutants. However, to further add to the complexity of enterococcal cell wall dynamics, L,D-

379 transpeptidases (LDTs), a novel class of enzymes that function apart from Pbps to promote penicillin
380 and cephalosporin, but not carbapenem resistance, may also contribute to this phenotype (42, 43). It is
381 possible that mutations in *sagA*, *epaR*, and/or *epaX* alter expression levels or post-translational
382 modification of Pbps or LDTs against ceftriaxone and ampicillin. An alternative hypothesis is that *sagA*,
383 *epaR*, and *epaX* gene mutations may manifest their effects through interaction with peptidoglycan and
384 the mechanism of enhanced β-lactam susceptibility may be exclusive from the activity of Pbps or LDTs.
385 Consistent with this notion, mutation of a secreted peptidoglycan hydrolase in *E. faecalis*, *salB*,
386 demonstrated enhanced susceptibility to cephalosporins. Pairwise amino acid alignment of *E. faecium*
387 Com12 SagA and *E. faecalis* SalB revealed 51% identity over the N-terminal coiled-coil domain region,
388 which is expected given their different C-terminal hydrolase domains (SCP in SalB; NlpC_P60 in
389 SagA). Contrary to *sagA* in *E. faecium*, *salB* was shown to be non-essential in *E. faecalis*, and has a
390 homolog (*salA*) which may partly compensate for the function of *salB* to maintain cell viability (24).
391 Staining of an *E. faecalis salB* mutant with a non-specific, fluorescent Pbp antibody (Bocillin FL)
392 revealed no difference from wild type. However, this analysis was performed in the absence of
393 ceftriaxone pre-treatment, potentially masking subtle changes in the abundance of Pbps in the *salB*
394 mutant at the cell wall (38). Therefore, it remains unclear if *salB* partners with or coordinates the activity
395 of Pbps or LDTs to induce cephalosporin resistance. A *sagA* mutant described in our study (81R5;
396 G460A) has a mutation residing two residues upstream from a peptidoglycan clamp residue (W462)
397 and lacked enhanced susceptibility to ampicillin and ceftriaxone. The reason for this exception and why
398 this mutation confers phage resistance is unclear.
399 The enhanced susceptibility to β-lactams in *epaR* and *epaX* in *E. faecium* mutants was
400 surprising given prior reports of increased β-lactam resistance in *epa* mutants in *E. faecalis* (44).
401 However, we note that all *epa* mutants tested in that analysis harbored mutations in genes from the
402 core region of *epa* locus (i.e. *epaA*, *epaE*, *epaL*, *epaN*, *epaB*). To the best of our knowledge, this is the
403 first report demonstrating enhanced β-lactam sensitivity to *epa* variable region mutants in enterococci.
404 We observed enhanced susceptibility to daptomycin in *E. faecium epaR* and *epaX* mutants, consistent
405 with data from *E. faecalis epaR* and *epaX* mutants (9, 14, 45). Given that the *epa* variable genes have

406 recently been discovered to be involved in teichoic acid biosynthesis (25), we hypothesize that altered
407 display of teichoic acids at the cell surface enables the differential β-lactam and daptomycin
408 susceptibility observed in *epa* core versus variable region mutants in enterococci. This hypothesis is
409 supported by observations in *Staphylococcus aureus*, where metabolic perturbations leading to
410 enhanced teichoic acid output or teichoic acid D-alanylation correlate with daptomycin tolerance (46-
411 48). Similarly, mutation of *lafB*, a gene encoding lipoteichoic acid glycosyltransferase, induces a
412 daptomycin hypersusceptible phenotype in *E. faecium* (49). Mutation of *bgsB* in *E. faecalis*, which
413 functions with a *lafB* homolog (*bgsA*) in lipoteichoic acid anchor biosynthesis, results in enhanced
414 susceptibility to daptomycin (14). A reduction in susceptibility to the β-lactam piperacillin in *lafB* (*E.*
415 *faecium*) or *bgsB* (*E. faecalis*) mutants is reminiscent of the effect of *epa* core region mutations in
416 enterococci (44). A similar pattern of enhanced daptomycin susceptibility at the cost of reduced β-
417 lactam susceptibility, known as the see-saw effect (50), suggests that the altered display or abundance
418 of the wall teichoic acids at the cell surface may occur in response to the modification of
419 rhamnopolysaccharide or lipoteichoic acid. Mutation of *epaR* or *epaX* in *E. faecium* would potentially
420 avoid the daptomycin-β-lactam see-saw effect, making phages that induce these mutations in
421 enterococci attractive antimicrobial candidates. Collectively, these observations suggest that the
422 location of *epa* mutations, core versus variable region, as well mutations in genes participating in
423 lipoteichoic acid biosynthesis, are likely to impact the trajectory of β-lactam and daptomycin
424 susceptibility in enterococci.
425 *E. faecalis epa* mutations are detrimental during intestinal colonization and show reduced
426 virulence in a mouse peritonitis infection model (9, 51, 52). *epa* mutants are more susceptible to bile
427 salts, neutrophils, exhibit reduced biofilm formation, and are unable to invade biotic and abiotic surfaces
428 (45, 52-54). Therefore, we predict that *epaR* and *epaX* mutants in *E. faecium* will show a similar
429 intestinal colonization dysfunction. Hydrolase-domain mutations in SagA are also likely to induce fitness
430 costs *in vivo*. SagA was shown to promote *E. faecium* attachment to multiple connective tissue
431 molecules, including fibrinogen, fibronectin, and collagen (23). Interestingly, peptidoglycan fragments
432 released following SagA hydrolytic activity activates NOD2-mediated mucosal immunity in the intestine,

433 providing protection from *Salmonella enterica* infection and *Clostridioides difficile* colitis (20, 22). In *E.*
434 *faecalis,* mutation of the *sagA*-like gene *salB* altered cell morphology, increased biofilm formation,
435 impacted autolysis, and increased susceptibility to bile salts, detergent, ethanol, peroxide, and heat (55-
436 58). Contrary to SagA, cells expressing SalB were limited in binding fibronectin and collagen type I,
437 suggesting that these proteins exhibit different adherence capacities to host tissue. Considering these
438 observations together, it is possible that phage predation that promotes the formation of *sagA* mutants
439 would result in *E. faecium* cells that are compromised for adherence and/or invasion of host tissues,
440 and potentially less immunostimulatory during infection.

441 In conclusion, we have identified three previously undescribed phages that infect *E. faecium.*
442 The study of *E. faecium* resistance to these phages identified multiple components of the *E. faecium*
443 cell surface to be critical for productive phage infection. The enhanced sensitivity of *sagA*, *epaR* and
444 *epaX* mutants to cell wall and membrane acting antimicrobials suggests that these proteins represent
445 intriguing antimicrobial targets to be considered for future drug discovery efforts against *E. faecium*, and
446 potentially other Gram-positive pathogens harboring homologs of these genes. The finding that *E.*
447 *faecium* phages synergize with β-lactam and lipopeptide antibiotics provides encouragement that
448 phages could be used in combination with these antibiotics to increase their efficacy and possibly
449 repurpose such antibiotics that are currently deemed ineffective against enterococci.
450

451 **Materials and Methods.**

452 **Bacteria and bacteriophages.** A complete list of the bacterial strains and bacteriophages used in this
453 study can be found in Table S4. *E. faecium* Com12 was cultured in Todd-Hewitt broth (THB) and *E.*
454 *faecium* 1,141,733 was cultured in brain heart infusion (BHI) broth at 37ºC with rotation at 250 rpm. *E.*
455 *coli* strains were cultured in Lennox L broth (LB) at 37ºC with rotation at 250 rpm. Semi-solid media in
456 petri plates were made by adding 1.5% agar to broth prior to autoclaving. For antibiotic susceptibility
457 testing, Mueller Hinton Broth (MHB) was used. When needed, chloramphenicol was added to media at
458 20 µg/ml or 10 µg/ml for selection of *E. coli* or *E. faecium*, respectively. Phage susceptibility assays
459 were performed on THB agar supplemented with 10mM $MgSO_4$.

460

461 **Bacteriophage isolation and purification.** Phages 9181, 9183, and 9184 were isolated from
462 wastewater obtained from a water treatment facility located near Denver, Colorado. Fifty milliliters of
463 raw sewage was centrifuged at 3220 x *g* for 10 minutes at room temperature to remove debris. The
464 supernatant was decanted and passed through a 0.45 µm filter. A 100µl aliquot of filtered wastewater
465 was mixed with 130 µl of *E. faecium* 1,141,733 or Com12 diluted 1:10 from an overnight culture and
466 incubated at room temperature for 15 min. Molten THB top agar (0.35%), supplemented with 10mM
467 $MgSO_4$, was added to the bacteria-wastewater suspension and poured over a 1.5% THB agar plate
468 supplemented with 10mM $MgSO_4$. Following overnight growth at 37ºC, plaques were picked with a
469 sterile Pasteur pipette and phages were eluted from the plaque in 500 µl SM-plus buffer (100 mM NaCl,
470 50 mM Tris-HCl, 8 mM $MgSO_4$, 5 mM $CaCl_2$ [pH 7.4]) overnight (O/N) at 4ºC. After O/N elution, the
471 phages were filter sterilized (0.45 µm). This procedure was repeated two more times to ensure clonal
472 phage isolates. To amplify phages to high titer stocks, 10-fold serially diluted clonal phage isolates were
473 mixed with their appropriate host strain diluted 1:10 from an O/N culture, incubated at room
474 temperature and then poured over 1.5% THB agar supplemented with 10mM $MgSO_4$. Top agar from
475 multiple near confluent lysed bacterial lawns were scraped into a 15 ml conical tube and centrifuged at
476 18000 x *g* for 10 minutes prior to decanting and 0.45 µm filter sterilization. Using these recovered
477 phages, high-titer phage stocks were generated by infecting 500mL of early logarithmically (2-3 x 10^8
478 CFU/mL) growing *E. faecium* with phage at a multiplicity of infection of 0.5 following supplementation of
479 media with 10mM $MgSO_4$. The phage-cell suspension was incubated at room temperature for 15 min
480 and then incubated at 37ºC with rotation (200 rpm) for 4-6 hours. The cultures were centrifuged at
481 3220 x *g* for 10 minutes at 4ºC and the supernatants filtered (0.45µm). Clarified and filtered lysates
482 were treated with 5 µg/ml each of DNase and RNase at room temperature for 1 hour and phages were
483 precipitated with 1M NaCl and 10% (wt/vol) polyethylene glycol 8000 (PEG 8000) on ice at 4ºC
484 overnight. Phage precipitates were pelleted by centrifugation at 11,270 x *g* for 20 minutes and
485 resuspended in 2mL of SM-plus buffer. One-third volume chloroform was mixed by inversion into the
486 phage precipitates and centrifuged at 16,300 x *g* to separate out residual PEG 8000 into the organic

487 phase. Phages in the aqueous phase were further purified using a cesium chloride gradient as
488 described previously (11). The final titer was confirmed by plaque assay. Crude phage lysates were
489 used for all phage susceptibility and adsorption assays, while cesium chloride gradient purified phages
490 were used for phage genomic DNA isolation and transmission electron microscopy.
491
492 **Transmission electron microscopy.** 8 µl of 1 x 10^{10} pfu/ml of phages was applied to a copper mesh
493 grid coated with formvar and carbon (Electron Microscopy Sciences) for 2 minutes and then gently
494 blotted off with a piece of Whatman filter paper. The grids were rinsed by transferring between two
495 drops of MilliQ water, blotting with Whatman filter paper between each transfer. Finally, the grids were
496 stained using two drops of a 0.75% uranyl formate solution (a quick rinse with MilliQ water following the
497 first drop followed by an additional 20 seconds of staining). After rinsing and blotting, the grids were
498 allowed to dry for at least 10 minutes. Samples were imaged on a FEI Tecnai G2 Biotwin TEM at 80kV
499 with an AMT side-mount digital camera.
500
501 **Whole-genome sequence analysis of phages and phage-resistant bacteria.** Phage DNA was
502 isolated by incubating phages with 50 µg/ml proteinase K and 0.5% sodium dodecyl sulfate at 56ºC for
503 1 hour followed by extraction with an equal volume of phenol/chloroform. The aqueous phase was
504 extracted a second time with an equal volume of chloroform and the DNA was precipitated using
505 isopropanol. Bacterial DNA was isolated using a ZymoBIOMICS DNA miniprep kit (Zymo Research),
506 following the manufacturers protocol. Phage and bacterial DNA samples were sequenced at the
507 Microbial Genome Sequencing Center, University of Pittsburgh, using an Illumina NextSeq 550 platform
508 and paired end chemistry (2 x 150bp). Paired-end reads were trimmed and assembled into contigs
509 using CLC genomics workbench (Qiagen). Open reading frames (ORFs) were detected and annotated
510 using rapid annotation subsystem technology (RAST) and the Phage Galaxy structural annotation
511 (version 2020.1) and functional workflows (version 2020.3) (59, 60). Trimmed bacterial genomic reads
512 for *E.* faecium Com12, 1,141,733, and phage resistant derivatives were mapped to reference genomes
513 (GCF_000157635.1 (Com12); GCA_000157575.1 (1,141,733)), downloaded from the National Center

514 for Biotechnology Information (NCBI) website. To identify mutations conferring phage resistance the
515 basic variant detection tool from CLC genomics workbench was used to identify polymorphisms
516 (similarity fraction = 0.5 and length fraction =0.8).
517
518 **Enterococcal phage orthology analysis.** Enterococcal phage orthology was performed according to
519 a method described by Bolocan et al. (16). Briefly, publicly available enterococcal genomes were
520 downloaded from the Millard Lab phage genome database (http://millardlab.org/bioinformatics/). As of
521 May 15, 2020, there were 99 complete enterococcal phage genomes. Open reading frames for each
522 enterococcal phage genome were called using Prodigal and bacteriophage protein Orthologous Groups
523 were identified by OrthoMCL (19, 61). The resulting OrthoMCL matrix was used to generate an
524 orthology tree using the ggplot2 and ggdendro packages in R. Nearest neighbor phages to phages
525 9181, 9183, and 9184 from the OrthoMCL analysis were compared using the genome alignment
526 feature of ViP Tree using normalized tBLASTx scores between viral genomes to calculate genomic
527 distance for phylogenetic proteomic tree analysis (62).
528
529 **Routine molecular techniques, DNA sequencing, and complementation.** Confirmation PCRs were
530 performed using GoTaq Green master mix (Promega), per the manufacturer's instructions. Q5 DNA
531 polymerase master mix (New England Biolabs) was used for PCR reactions intended for cloning, per
532 the manufacturer's instructions. Plasmid DNA was purified using a QIAprep Miniprep kit (Qiagen) or a
533 ZymoPURE II Plasmid Midiprep kit (Zymo Research). Restriction enzymes and T4 ligase were
534 purchased from New England Biolabs. Sanger DNA sequencing was performed by Quintara
535 Biosciences (San Francisco, CA). A complete list of primers can be found in Table S4.
536 Complementation was performed using plasmid pLZ12A, a derivative of pLZ12 (63) carrying the *bacA*
537 promoter upstream of the multiple cloning site (9). *wze*, *epaX*, *dltA*, and *efsg_rs08090* were cloned into
538 pLZ12A as BamHI and EcoRI fragments. *epaR* and *efsg_rs08120* were cloned into pLZ12A as BamHI
539 and PstI fragments. Plasmids were transformed into *E. faecium* using a previously described glycine-
540 sucrose method (64, 65). Briefly, 1ml of overnight culture was inoculated into 50ml of BHI

541 supplemented with 2% glycine and 0.5M sucrose and grown overnight at 37°C with rotation (250 rpm).
542 The following day the cells were pelleted at 7200 x *g* and re-suspended in an equal volume of pre-
543 warmed BHI supplemented with 2% glycine and 0.5M sucrose and incubated for 1h at 37°C statically.
544 The cells were pelleted at 7200 x *g* and washed three times in ice cold electroporation buffer (0.5M
545 sucrose and 10% glycerol). 1-2 µg of plasmid DNA was electroporated into *E. faecium* using a Gene
546 Pulser (Bio-Rad) with a 0.2 mm cuvette at 1.7kV, 200 Ω and 25 µF.
547
548 **Phage susceptibility assay.** Overnight bacterial cultures were pelleted, resuspended in SM-plus
549 buffer, and normalized to OD_{600} of 1.0. 10-fold serial dilutions of bacteria were spotted on THB agar
550 embedded with phage or THB agar alone, supplemented with 10mM $MgSO_4$. Phages were embedded
551 at the following concentrations within THB agar: phage 9181 (10^8 PFU/ml), phage 9183 (10^7 PFU/ml),
552 and phage 9184 (10^7 PFU/ml). Plates were incubated overnight at 37°C and viable CFU was
553 determined by colony counting.
554
555 **Isolation of phage-resistant *E. faecium* strains.** 130 µl of a 1:10 dilution of *E. faecium* grown O/N
556 was mixed with 10 µl of 10-fold serially diluted phages and added to 5 ml of prewarmed THB top agar
557 (0.35% wt/vol). Phage-bacterium mixtures were poured onto the surface of THB agar plates (1.5%
558 wt/vol). The plates were incubated at 37°C until phage-resistant colonies appeared in the zones of
559 clearing. The presumptive resistant colonies were passaged four times by streaking single colonies
560 onto THB agar.
561
562 **Determination of phage host range.** The host range of phages 9181, 9183, and 9184 were
563 determined using a panel of laboratory and contemporary clinical *E. faecium* and *E. faecalis* isolates
564 (Table S4). Overnight bacterial cultures were suspended in SM-plus buffer to an OD_{600} of 1.0 and 10-
565 fold serially diluted and spotted on to THB agar containing phages. Plates were incubated O/N at 37°C
566 and viable CFU was determined. Strains that exhibited greater than 4-log killing in the presence of

567 phage were termed phage susceptible, while those that grew beyond this threshold were considered
568 phage resistant.
569
570 **Phage adsorption assay.** This assay was performed as described previously (10, 11). O/N bacterial
571 cultures were pelleted at 3220 × *g* for 10 min and resuspended to 10^8 CFU/ml in SM-plus buffer. Phage
572 adsorption was determined by mixing 5 x 10^6 pfu of phage and to 5 x 10^7 cfu of the appropriate
573 bacterial strain in 500 µl and incubating statically at room temperature for 10 min. The bacteria-phage
574 suspensions were centrifuged at 24,000 × *g* for 1 min, the supernatant was collected, and remaining
575 phages enumerated by a plaque assay. SM-plus buffer with phage only (no bacteria) served as a
576 control. Percent adsorption was determined as follows: $[(PFU_{control} - PFU_{test\ supernatant})/PFU_{control}] \times 100$.
577 The fold change was calculated by dividing the percent adsorption of phage resistant mutants by those
578 of parental strain.
579
580 **Antibiotic MIC assay.** Antibiotic MIC was determined for each strain using Etest strips (bioMérieux).
581 Single colonies were grown O/N in 3mL of MHB broth at 37ºC with rotation (250 rpm). The following
582 day overnight cultures were diluted to McFarland 0.5 in MHB broth and 100µL of the cell suspension
583 was spread over the surface of MHB agar plates. One Etest strip was placed on the surface of the agar
584 using sterile forceps. The plates were incubated for 18 hours at 37ºC. The MIC was determined to be
585 the number closest to the zone of inhibition. The MIC reported for each strain is representative of two
586 independent experiments.
587
588 **Phage-antibiotic synergy assay.** O/N cultures of *E. faecium* Com12 and *E. faecium* 1,141,733 were
589 normalized to 10^8 CFU/mL. 100µl (10^7 CFU/mL) of bacteria was added into a sterile 96-well plate
590 (Falcon) in triplicate. Antibiotics were diluted 1:100 into desired wells to achieve the appropriate final
591 concentration. Phages were added to desired wells at 10^6 PFU/ml, achieving a multiplicity of infection
592 of 0.1. The 96 well plate was loaded on to BioTek Synergy Plate reader pre-warmed to 37ºC, and
593 agitated continuously for 18h, allowing for OD_{600} reading every 30 minutes.

594

595 **Data availability.** The Illumina reads for phage 9181, 9183, and 9184 and phage-resistant *E. faecium*
596 mutants have been deposited in the European Nucleotide Archive under the accession number
597 PRJEB39873. Assembled phage genomes were submitted to Genbank and were assigned the
598 following accession numbers: MT939240 (phage 9181), MT939241 (phage 9183), and MT939242
599 (phage 9184).

600

601 **Acknowledgements.**

602 This work was supported by National Institutes of Health grants R01AI141479 (B.A.D.). We thank Dr.
603 Jennifer Bourne at the University of Colorado School of Medicine Electron Microscopy Center for
604 preparing and visualizing electron micrographs of phages. We thank the staff at the Microbial Genome
605 Sequencing Center (MiGS) at the University of Pittsburgh for assistance with bacterial and phage whole
606 genome DNA sequencing. We thank Dr. Howard Hang and Juliel Espinosa for generously providing
607 pAM401-*sagA*.

608

609 **References.**

610 1. Arias CA, Murray BE. 2012. The rise of the Enterococcus: beyond vancomycin
611 resistance. Nat Rev Microbiol 10:266-78.
612 2. Kristich CJ, Rice LB, Arias CA. 2014. Enterococcal infection—treatment and antibiotic
613 resistance, p 1-62. *In* Gilmore MS, Clewell DB, Ike Y, Shakar N (ed), Enterococci : from
614 commensals to leading causes of drug resistant infection [Internet]. Massachusetts Eye
615 and Ear Infirmary, Boston, MA.
616 3. Beganovic M, Luther MK, Rice LB, Arias CA, Rybak MJ, LaPlante KL. 2018. A review of
617 combination antimicrobial therapy for *Enterococcus faecalis* bloodstream infections and
618 infective endocarditis. Clin Infect Dis 67:303-309.
619 4. Rybak MJ, McGrath BJ. 1996. Combination antimicrobial therapy for bacterial
620 infections. Guidelines for the clinician. Drugs 52:390-405.
621 5. Fish R, Kutter E, Bryan D, Wheat G, Kuhl S. 2018. Resolving digital staphylococcal
622 osteomyelitis using bacteriophage-a case report. Antibiotics (Basel) 7.
623 6. Cano EJ, Caflisch KM, Bollyky PL, Van Belleghem JD, Patel R, Fackler J, Brownstein
624 MJ, Horne B, Biswas B, Henry M, Malagon F, Lewallen DG, Suh GA. 2020. Phage
625 therapy for limb-threatening prosthetic knee *Klebsiella pneumoniae* infection: case
626 report and in vitro characterization of anti-biofilm activity. Clin Infect Dis
627 doi:10.1093/cid/ciaa705.

628 7. Schooley RT, Biswas B, Gill JJ, Hernandez-Morales A, Lancaster J, Lessor L, Barr JJ,
629 Reed SL, Rohwer F, Benler S, Segall AM, Taplitz R, Smith DM, Kerr K, Kumaraswamy
630 M, Nizet V, Lin L, McCauley MD, Strathdee SA, Benson CA, Pope RK, Leroux BM, Picel
631 AC, Mateczun AJ, Cilwa KE, Regeimbal JM, Estrella LA, Wolfe DM, Henry MS,
632 Quinones J, Salka S, Bishop-Lilly KA, Young R, Hamilton T. 2017. Development and
633 use of personalized bacteriophage-based therapeutic cocktails to treat a patient with a
634 disseminated resistant *Acinetobacter baumannii* infection. Antimicrob Agents
635 Chemother 61.
636 8. Chan BK, Turner PE, Kim S, Mojibian HR, Elefteriades JA, Narayan D. 2018. Phage
637 treatment of an aortic graft infected with Pseudomonas aeruginosa. Evol Med Public
638 Health 2018:60-66.
639 9. Chatterjee A, Johnson CN, Luong P, Hullahalli K, McBride SW, Schubert AM, Palmer
640 KL, Carlson PE, Jr., Duerkop BA. 2019. Bacteriophage resistance alters antibiotic-
641 mediated intestinal expansion of enterococci. Infect Immun 87.
642 10. Chatterjee A, Willett JLE, Nguyen UT, Monogue B, Palmer KL, Dunny GM, Duerkop BA.
643 2020. Parallel genomics uncover novel enterococcal-bacteriophage interactions. mBio
644 11.
645 11. Duerkop BA, Huo W, Bhardwaj P, Palmer KL, Hooper LV. 2016. Molecular basis for lytic
646 bacteriophage resistance in enterococci. mBio 7.
647 12. Wandro S, Oliver A, Gallagher T, Weihe C, England W, Martiny JBH, Whiteson K. 2018.
648 Predictable molecular adaptation of coevolving *Enterococcus faecium* and lytic phage
649 EfV12-phi1. Front Microbiol 9:3192.
650 13. Lossouarn J, Briet A, Moncaut E, Furlan S, Bouteau A, Son O, Leroy M, DuBow MS,
651 Lecointe F, Serror P, Petit MA. 2019. *Enterococcus faecalis* countermeasures defeat a
652 virulent Picovirinae bacteriophage. Viruses 11.
653 14. Ho K, Huo W, Pas S, Dao R, Palmer KL. 2018. Loss-of-function mutations in *epaR*
654 confer resistance to phiNPV1 Infection in *Enterococcus faecalis* OG1RF. Antimicrob
655 Agents Chemother 62.
656 15. Duerkop BA, Palmer KL, Horsburgh MJ. 2014. Enterococcal bacteriophages and
657 genome defense. *In* Gilmore MS, Clewell DB, Ike Y, Shankar N (ed), Enterococci: from
658 commensals to leading causes of drug resistant infection. Massachusetts Eye and Ear
659 Infirmary, Boston.
660 16. Bolocan AS, Upadrasta A, Bettio PHA, Clooney AG, Draper LA, Ross RP, Hill C. 2019.
661 Evaluation of phage therapy in the context of *Enterococcus faecalis* and its associated
662 diseases. Viruses 11.
663 17. Palmer KL, Godfrey P, Griggs A, Kos VN, Zucker J, Desjardins C, Cerqueira G, Gevers
664 D, Walker S, Wortman J, Feldgarden M, Haas B, Birren B, Gilmore MS. 2012.
665 Comparative genomics of enterococci: variation in *Enterococcus faecalis*, clade
666 structure in *E. faecium*, and defining characteristics of *E. gallinarum* and *E.*
667 *casseliflavus*. mBio 3:e00318-11.
668 18. Ackermann HW. 2007. 5500 Phages examined in the electron microscope. Arch Virol
669 152:227-43.
670 19. Li L, Stoeckert CJ, Jr., Roos DS. 2003. OrthoMCL: identification of ortholog groups for
671 eukaryotic genomes. Genome Res 13:2178-89.
672 20. Kim B, Wang YC, Hespen CW, Espinosa J, Salje J, Rangan KJ, Oren DA, Kang JY,
673 Pedicord VA, Hang HC. 2019. *Enterococcus faecium* secreted antigen A generates
674 muropeptides to enhance host immunity and limit bacterial pathogenesis. Elife 8.

675 21. Ittisoponpisan S, Islam SA, Khanna T, Alhuzimi E, David A, Sternberg MJE. 2019. Can
676 predicted protein 3D structures provide reliable insights into whether missense variants
677 are disease associated? J Mol Biol 431:2197-2212.
678 22. Rangan KJ, Pedicord VA, Wang YC, Kim B, Lu Y, Shaham S, Mucida D, Hang HC.
679 2016. A secreted bacterial peptidoglycan hydrolase enhances tolerance to enteric
680 pathogens. Science 353:1434-1437.
681 23. Teng F, Kawalec M, Weinstock GM, Hryniewicz W, Murray BE. 2003. An *Enterococcus*
682 *faecium* secreted antigen, SagA, exhibits broad-spectrum binding to extracellular matrix
683 proteins and appears essential for *E. faecium* growth. Infect Immun 71:5033-41.
684 24. Djoric D, Kristich CJ. 2017. Extracellular SalB contributes to intrinsic cephalosporin
685 resistance and cell envelope integrity in *Enterococcus faecalis*. J Bacteriol 199.
686 25. Guerardel Y, Sadovskaya I, Maes E, Furlan S, Chapot-Chartier MP, Mesnage S,
687 Rigottier-Gois L, Serror P. 2020. Complete structure of the enterococcal polysaccharide
688 antigen (EPA) of vancomycin-resistant *Enterococcus faecalis* V583 Reveals that EPA
689 decorations are teichoic acids covalently linked to a rhamnopolysaccharide backbone.
690 mBio 11.
691 26. Kortright KE, Chan BK, Koff JL, Turner PE. 2019. Phage therapy: a renewed approach
692 to combat antibiotic-resistant bacteria. Cell Host Microbe 25:219-232.
693 27. Mangalea MR, Duerkop BA. 2020. Fitness trade-offs resulting from bacteriophage
694 resistance potentiate synergistic antibacterial strategies. Infect Immun 88.
695 28. Morrisette T, Lev KL, Kebriaei R, Abdul-Mutakabbir J, Stamper KC, Morales S, Lehman
696 SM, Canfield GS, Duerkop BA, Arias CA, Rybak MJ. 2020. Bacteriophage-antibiotic
697 combinations for *Enterococcus faecium* with varying bacteriophage and daptomycin
698 susceptibilities. Antimicrob Agents Chemother doi:10.1128/AAC.00993-20.
699 29. Rice LB, Lakticová V, Helfand MS, Hutton-Thomas R. 2004. In vitro antienterococcal
700 activity explains associations between exposures to antimicrobial agents and risk of
701 colonization by multiresistant enterococci. J Infect Dis 190:2162-6.
702 30. Ubeda C, Taur Y, Jenq RR, Equinda MJ, Son T, Samstein M, Viale A, Socci ND, van
703 den Brink MR, Kamboj M, Pamer EG. 2010. Vancomycin-resistant *Enterococcus*
704 domination of intestinal microbiota is enabled by antibiotic treatment in mice and
705 precedes bloodstream invasion in humans. J Clin Invest 120:4332-41.
706 31. Brandl K, Plitas G, Mihu CN, Ubeda C, Jia T, Fleisher M, Schnabl B, DeMatteo RP,
707 Pamer EG. 2008. Vancomycin-resistant enterococci exploit antibiotic-induced innate
708 immune deficits. Nature 455:804-7.
709 32. Donskey CJ, Chowdhry TK, Hecker MT, Hoyen CK, Hanrahan JA, Hujer AM, Hutton-
710 Thomas RA, Whalen CC, Bonomo RA, Rice LB. 2000. Effect of antibiotic therapy on the
711 density of vancomycin-resistant enterococci in the stool of colonized patients. N Engl J
712 Med 343:1925-32.
713 33. Hendrickx AP, Top J, Bayjanov JR, Kemperman H, Rogers MR, Paganelli FL, Bonten
714 MJ, Willems RJ. 2015. Antibiotic-driven dysbiosis mediates intraluminal agglutination
715 and alternative segregation of *Enterococcus faecium* from the intestinal epithelium.
716 mBio 6:e01346-15.
717 34. Duan Y, Llorente C, Lang S, Brandl K, Chu H, Jiang L, White RC, Clarke TH, Nguyen K,
718 Torralba M, Shao Y, Liu J, Hernandez-Morales A, Lessor L, Rahman IR, Miyamoto Y,
719 Ly M, Gao B, Sun W, Kiesel R, Hutmacher F, Lee S, Ventura-Cots M, Bosques-Padilla
720 F, Verna EC, Abraldes JG, Brown RS, Jr., Vargas V, Altamirano J, Caballeria J,
721 Shawcross DL, Ho SB, Louvet A, Lucey MR, Mathurin P, Garcia-Tsao G, Bataller R, Tu
722 XM, Eckmann L, van der Donk WA, Young R, Lawley TD, Starkel P, Pride D, Fouts DE,

723 Schnabl B. 2019. Bacteriophage targeting of gut bacterium attenuates alcoholic liver
724 disease. Nature 575:505-511.
725 35. Stein-Thoeringer CK, Nichols KB, Lazrak A, Docampo MD, Slingerland AE, Slingerland
726 JB, Clurman AG, Armijo G, Gomes ALC, Shono Y, Staffas A, Burgos da Silva M, Devlin
727 SM, Markey KA, Bajic D, Pinedo R, Tsakmaklis A, Littmann ER, Pastore A, Taur Y,
728 Monette S, Arcila ME, Pickard AJ, Maloy M, Wright RJ, Amoretti LA, Fontana E, Pham
729 D, Jamal MA, Weber D, Sung AD, Hashimoto D, Scheid C, Xavier JB, Messina JA,
730 Romero K, Lew M, Bush A, Bohannon L, Hayasaka K, Hasegawa Y, Vehreschild M,
731 Cross JR, Ponce DM, Perales MA, Giralt SA, Jenq RR, Teshima T, Holler E, Chao NJ,
732 et al. 2019. Lactose drives *Enterococcus* expansion to promote graft-versus-host
733 disease. Science 366:1143-1149.
734 36. Baddour LM, Wilson WR, Bayer AS, Fowler VG, Jr., Tleyjeh IM, Rybak MJ, Barsic B,
735 Lockhart PB, Gewitz MH, Levison ME, Bolger AF, Steckelberg JM, Baltimore RS, Fink
736 AM, O'Gara P, Taubert KA, American Heart Association Committee on Rheumatic
737 Fever E, Kawasaki Disease of the Council on Cardiovascular Disease in the Young
738 CoCCCoCS, Anesthesia, Stroke C. 2015. Infective endocarditis in adults: diagnosis,
739 antimicrobial therapy, and management of complications: a scientific statement for
740 healthcare professionals from the American Heart Association. Circulation 132:1435-86.
741 37. Lorenzo MP, Kidd JM, Jenkins SG, Nicolau DP, Housman ST. 2019. In vitro activity of
742 ampicillin and ceftriaxone against ampicillin-susceptible *Enterococcus faecium*. J
743 Antimicrob Chemother 74:2269-2273.
744 38. Djoric D, Little JL, Kristich CJ. 2020. Multiple low-reactivity class B penicillin-binding
745 proteins are required for cephalosporin resistance in enterococci. Antimicrob Agents
746 Chemother 64.
747 39. Arbeloa A, Segal H, Hugonnet JE, Josseaume N, Dubost L, Brouard JP, Gutmann L,
748 Mengin-Lecreulx D, Arthur M. 2004. Role of class A penicillin-binding proteins in PBP5-
749 mediated beta-lactam resistance in Enterococcus faecalis. J Bacteriol 186:1221-8.
750 40. Rice LB, Carias LL, Rudin S, Hutton R, Marshall S, Hassan M, Josseaume N, Dubost L,
751 Marie A, Arthur M. 2009. Role of class A penicillin-binding proteins in the expression of
752 beta-lactam resistance in *Enterococcus faecium*. J Bacteriol 191:3649-56.
753 41. Sifaoui F, Arthur M, Rice L, Gutmann L. 2001. Role of penicillin-binding protein 5 in
754 expression of ampicillin resistance and peptidoglycan structure in *Enterococcus*
755 *faecium*. Antimicrob Agents Chemother 45:2594-7.
756 42. Triboulet S, Dubee V, Lecoq L, Bougault C, Mainardi JL, Rice LB, Etheve-Quelquejeu
757 M, Gutmann L, Marie A, Dubost L, Hugonnet JE, Simorre JP, Arthur M. 2013. Kinetic
758 features of L,D-transpeptidase inactivation critical for beta-lactam antibacterial activity.
759 PLoS One 8:e67831.
760 43. Mainardi JL, Hugonnet JE, Rusconi F, Fourgeaud M, Dubost L, Moumi AN, Delfosse V,
761 Mayer C, Gutmann L, Rice LB, Arthur M. 2007. Unexpected inhibition of peptidoglycan
762 LD-transpeptidase from *Enterococcus faecium* by the beta-lactam imipenem. J Biol
763 Chem 282:30414-22.
764 44. Singh KV, Murray BE. 2019. Loss of a major enterococcal polysaccharide antigen (Epa)
765 by *Enterococcus faecalis* is associated with increased resistance to ceftriaxone and
766 carbapenems. Antimicrob Agents Chemother 63.
767 45. Dale JL, Cagnazzo J, Phan CQ, Barnes AM, Dunny GM. 2015. Multiple roles for
768 *Enterococcus faecalis* glycosyltransferases in biofilm-associated antibiotic resistance,
769 cell envelope integrity, and conjugative transfer. Antimicrob Agents Chemother 59:4094-
770 105.

771 46. Gaupp R, Lei S, Reed JM, Peisker H, Boyle-Vavra S, Bayer AS, Bischoff M, Herrmann
772 M, Daum RS, Powers R, Somerville GA. 2015. *Staphylococcus aureus* metabolic
773 adaptations during the transition from a daptomycin susceptibility phenotype to a
774 daptomycin nonsusceptibility phenotype. Antimicrob Agents Chemother 59:4226-38.
775 47. Mechler L, Bonetti EJ, Reichert S, Flotenmeyer M, Schrenzel J, Bertram R, Francois P,
776 Gotz F. 2016. Daptomycin tolerance in the *Staphylococcus aureus pitA6* mutant is due
777 to upregulation of the *dlt* operon. Antimicrob Agents Chemother 60:2684-91.
778 48. Bertsche U, Weidenmaier C, Kuehner D, Yang SJ, Baur S, Wanner S, Francois P,
779 Schrenzel J, Yeaman MR, Bayer AS. 2011. Correlation of daptomycin resistance in a
780 clinical *Staphylococcus aureus* strain with increased cell wall teichoic acid production
781 and D-alanylation. Antimicrob Agents Chemother 55:3922-8.
782 49. Mello SS, Van Tyne D, Lebreton F, Silva SQ, Nogueira MCL, Gilmore MS, Camargo I.
783 2020. A mutation in the glycosyltransferase gene *lafB* causes daptomycin
784 hypersusceptibility in *Enterococcus faecium*. J Antimicrob Chemother 75:36-45.
785 50. Sieradzki K, Tomasz A. 1997. Inhibition of cell wall turnover and autolysis by
786 vancomycin in a highly vancomycin-resistant mutant of *Staphylococcus aureus*. Journal
787 of Bacteriology 179:2557-2566.
788 51. Xu Y, Singh KV, Qin X, Murray BE, Weinstock GM. 2000. Analysis of a gene cluster of
789 *Enterococcus faecalis* involved in polysaccharide biosynthesis. Infect Immun 68:815-23.
790 52. Rigottier-Gois L, Madec C, Navickas A, Matos RC, Akary-Lepage E, Mistou MY, Serror
791 P. 2015. The surface rhamnopolysaccharide epa of *Enterococcus faecalis* is a key
792 determinant of intestinal colonization. J Infect Dis 211:62-71.
793 53. Mohamed JA, Huang W, Nallapareddy SR, Teng F, Murray BE. 2004. Influence of origin
794 of isolates, especially endocarditis isolates, and various genes on biofilm formation by
795 *Enterococcus faecalis*. Infect Immun 72:3658-63.
796 54. Ramos Y, Rocha J, Hael AL, van Gestel J, Vlamakis H, Cywes-Bentley C, Cubillos-Ruiz
797 JR, Pier GB, Gilmore MS, Kolter R, Morales DK. 2019. PolyGlcNAc-containing
798 exopolymers enable surface penetration by non-motile *Enterococcus faecalis*. PLoS
799 Pathog 15:e1007571.
800 55. Breton YL, Mazé A, Hartke A, Lemarinier S, Auffray Y, Rincé A. 2002. Isolation and
801 characterization of bile salts-sensitive mutants of *Enterococcus faecalis*. Current
802 Microbiology 45:0434-0439.
803 56. Rincé A, Le Breton Y, Verneuil N, Giard J-C, Hartke A, Auffray Y. 2003. Physiological
804 and molecular aspects of bile salt response in *Enterococcus faecalis*. International
805 Journal of Food Microbiology 88:207-213.
806 57. Mohamed JA, Teng F, Nallapareddy SR, Murray BE. 2006. Pleiotrophic effects of 2
807 *Enterococcus faecalis sagA*-like genes, *salA* and *salB*, which encode proteins that are
808 antigenic during human infection, on biofilm formation and binding to collagen type i and
809 fibronectin. J Infect Dis 193:231-40.
810 58. Shankar J, Walker RG, Wilkinson MC, Ward D, Horsburgh MJ. 2012. SalB inactivation
811 modulates culture supernatant exoproteins and affects autolysis and viability in
812 *Enterococcus faecalis* OG1RF. J Bacteriol 194:3569-78.
813 59. Aziz RK, Bartels D, Best AA, DeJongh M, Disz T, Edwards RA, Formsma K, Gerdes S,
814 Glass EM, Kubal M, Meyer F, Olsen GJ, Olson R, Osterman AL, Overbeek RA, McNeil
815 LK, Paarmann D, Paczian T, Parrello B, Pusch GD, Reich C, Stevens R, Vassieva O,
816 Vonstein V, Wilke A, Zagnitko O. 2008. The RAST Server: rapid annotations using
817 subsystems technology. BMC Genomics 9:75.
818 60. Mijalis E, Rasche H. 2013-2017. CPT galaxy tools. https://github.com/tamu-cpt/galaxy-
819 tools/ Accessed 1 May 2020.

820 61. Hyatt D, Chen GL, Locascio PF, Land ML, Larimer FW, Hauser LJ. 2010. Prodigal:
821 prokaryotic gene recognition and translation initiation site identification. BMC
822 Bioinformatics 11:119.
823 62. Nishimura Y, Yoshida T, Kuronishi M, Uehara H, Ogata H, Goto S. 2017. ViPTree: the
824 viral proteomic tree server. Bioinformatics 33:2379-2380.
825 63. Perez-Casal J, Caparon MG, Scott JR. 1991. Mry, a trans-acting positive regulator of
826 the M protein gene of *Streptococcus pyogenes* with similarity to the receptor proteins of
827 two-component regulatory systems. J Bacteriol 173:2617-24.
828 64. Shepard BD, Gilmore MS. 1995. Electroporation and efficient transformation of
829 *Enterococcus faecalis* grown in high concentrations of glycine. Methods Mol Biol
830 47:217-26.
831 65. Zhang X, Paganelli FL, Bierschenk D, Kuipers A, Bonten MJ, Willems RJ, van Schaik
832 W. 2012. Genome-wide identification of ampicillin resistance determinants in
833 *Enterococcus faecium*. PLoS Genet 8:e1002804.
834 66. Mihara T, Nishimura Y, Shimizu Y, Nishiyama H, Yoshikawa G, Uehara H, Hingamp P,
835 Goto S, Ogata H. 2016. Linking virus genomes with host taxonomy. Viruses 8:66.
836

837 **Figure Legends.**

838 **Figure 1. Genome organization and morphogenesis of three previously uncharacterized *E.***
839 ***faecium* phages.** Whole genome sequencing reveals a modular functional organization of phage
840 9181, 9183 and 9184 genomes. Open reading frames for each phage were determined by RAST
841 version 2.0 and by the Texas A&M Center for Phage Therapy structural analysis workflow version
842 2020.01. Colored open reading frames correspond to the functional prediction. Beneath the phage
843 genome maps, TEM shows phage 9181, 9183 and 9184 are non-contractile tailed *Siphoviridae*. The *E.*
844 *faecium* host strain for phage 9181 is *E. faecium* Com12. The host strain for phage 9183 and 9184 is
845 *E. faecium* 1,141,733.

846

847 **Figure 2. Comparative genomic analysis identifies two novel enterococcal phage orthoclusters.**
848 A comparative genome analysis was performed using OrthoMCL as described previously by Bolocan et
849 al. (16). A phylogenetic proteomic tree was constructed from the OrthoMCL matrix using the Manhattan
850 distance metric and hierarchical clustering using an average linkage with 1000 iterations. Ninety-nine
851 enterococcal phage genomes available from NCBI were used for comparison to *E. faecium* phages
852 9181, 9183, and 9184 (highlighted in red). Distinct phage orthoclusters are represented by colored
853 boxes. Roman numerals to the right of the shaded boxes signify the phage orthocluster number. Phage

854 orthocluster morphology is indicated by calipers (if known) or an asterisk symbol (if unknown) to the
855 right of the roman numerals.
856
857 **Figure 3. *E. faecium* phages demonstrate broad and narrow host ranges.** Host ranges of phage
858 9181, 9183, and 9184. Phage 9181 and 9183 have a narrow *E. faecium* host range, while phage 9184
859 shows a broader host range. Bacteria were susceptible if less than 1 x 10^5 CFU/mL of bacteria were
860 recovered from a phage susceptibility assay. Bacteria were resistant if greater than 1 x 10^5 CFU/mL of
861 bacteria were recovered from a phage susceptibility assay. (A) Indicates host range for a collection of
862 laboratory strains. (B) Indicates the host range for a collection of clinical isolates provided by the clinical
863 microbiology lab at the University of Colorado, Anschutz Medical Campus.
864
865 **Figure 4. *E. faecium* elicits a robust resistance phenotype to phage 9181 and 9183, but variable**
866 **resistance to phage 9184.** Representative phage resistant strains raised against phages 9181 (A),
867 9183 (B), and 9184 (C). Data show phage susceptibility assays and associated bacterial enumeration
868 of wild type and phage resistant mutants in the presence (white bars) or absence (black bars) of phage
869 from three independent experiments. Error bars indicate standard deviation. Phage 9181 resistant (A)
870 and phage 9183 resistant (B) strains exhibit ≥ 4-log of survival in the presence of phages compared to
871 the parental *E. faecium* Com12 and 1,141,733 (733) strains, respectively. Phage 9184 resistant strains
872 (C) exhibit diverse resistance strength characterized weak (84R2) and strong (84R6) resistance
873 phenotypes. The dotted line indicates the spontaneous mutation threshold conferring phage resistance
874 observed in the respective wild type host strain of each phage.
875
876 **Figure 5. A diverse assortment of mutations confer phage resistance in *E. faecium*.** (A) Protein
877 secondary structure of *E. faecium* Com12 SagA, consisting of an N-terminus coiled-coil domain
878 (residues 18-242) and C-terminus NlpC_P60 peptidoglycan hydrolase domain (residues 393-520).
879 Displayed above the protein structure are colored lollipops denoting the site of mutations within
880 NlpC_P60 domain of phage 9181-resistant mutants. Inside and below the protein structure are colored

881 one letter amino acid abbreviations and lines, respectively, corresponding to key active site (red) and
882 peptidoglycan clamp residues (teal) of the NlpC_P60 domain. Abbreviations: W, tryptophan; C,
883 Cysteine; H, Histidine; G, Glycine; D, Aspartate; L, Leucine; Y, Tyrosine; V, Valine. (B) Capsule locus
884 mutations are detected in a tyrosine kinase (*wze*), aminotransferase (*efsg_rs08090*), *wzy*
885 (*efsg_rs08105*), and nucleotide sugar dehydrogenase (*efsg_rs08120*) of phage 9184-resistant mutants.
886 Arrows indicate open reading frames. Arrow colors correspond to colored boxes (figure bottom left)
887 indicate predicted open reading frame function (17). Colored lollipops above the arrows corresponding
888 to colored dots (figure bottom right) indicate the mutational type. *E. faecium* 1,141,733 locus tags are
889 angled below the arrows. (C) A missense mutation is found within a predicted arginine-aspartate-
890 aspartate protein (*rdd*; black arrow) of one phage 9184-resistant mutant (84R6) of *E. faecium*
891 1,141,733. *rdd* is flanked upstream by a predicted hypothetical protein (white arrow) and signal
892 sequence peptidase A (*sspA*; black arrow) and downstream by another hypothetical protein (white
893 arrow). *E. faecium* 1,141,733 locus tags are angled below the arrows. (D) Mutations in predicted
894 teichoic acid biosynthesis genes (*epaR* and *epaX*) are identified in phage 9183-resistant mutants of *E.*
895 *faecium* 1,141,733 (25). Arrow colors correspond to colored boxes (figure bottom left) indicate
896 predicted open reading frame function. Colored lollipops above the arrows corresponding to colored
897 dots (figure bottom right) indicate the mutational type. *E. faecium* 1,141,733 locus tags are angled
898 below the arrows. The brackets above the locus correspond the conserved (left) and variable (right)
899 portions of the *epa* locus proposed to by Gueredal et al. to encode the machinery necessary for
900 rhamnopolysaccharide synthesis and wall teichoic acid biosynthesis, respectively (25).
901
902 **Figure 6. Mutation in the capsule and exopolysaccharide loci limit phage adsorption in *E.***
903 ***faecium*.** Shown is the fold-change in phage 9181 (A), 9183 (B), and 9184 (C) adsorption compared to
904 wild type (WT) *E. faecium*. Results represent average fold-change and standard deviation from three
905 independent experiments. *, $P < 0.05$; **, $P < 0.01$ using an unpaired Student's *t* test.
906

907 **Figure 7. Phage 9181 and phage 9183 synergize with antibiotics to kill *E. faecium*.** (A-E) *E.*
908 *faecium* growth was monitored over 18 hours in the presence of phage (open blue squares), sub-
909 inhibitory concentrations of antibiotics (open orange, grey, purple triangles or diamonds), both phage
910 and sub-inhibitory concentration of antibiotics (filled orange, grey and purple triangles or diamonds), or
911 media alone (open black circles). Phage 9181 was used in experiments with *E. faecium* Com12, while
912 phage 9183 was employed for experiments with 1,141,733. Phages 9181 (A) and 9183 (B) synergize
913 with sub-inhibitory concentration of ampicillin (AMP) in a dose responsive manner to kill *E. faecium*
914 Com12 and 1,141,733, respectively. Phage 9181 (C) and 9183 (D) synergize with sub-inhibitory
915 concentrations of ceftriaxone (CTX) to kill *E. faecium* Com12 and 1,141,733, respectively. Phage 9183
916 (E) synergizes with sub-inhibitory concentrations of daptomycin (DAP) in a dose-responsive manner to
917 kill *E. faecium* 1,141,733. Three technical replicates were performed for each condition tested and the
918 averages plotted. Error bars indicate standard deviation. Shown are the results from one experiment
919 that was replicated in triplicate.
920
921 **Supplemental Figure Legends**
922 **Figure S1. *Enterococcus faecium* phage orthoclusters.** Phage protein coding sequence alignments
923 were performed with nearest neighbors in VIP Tree (62, 66). Colored lines connecting genomes
924 indicate percent protein identity along the length of each genome. (A) Phage 9183 demonstrates
925 protein homology and similar genome organization to its nearest neighbor intra-orthocluster phages
926 (phages VFW and VPE25). (B) Phage 9184 demonstrates proteome homology and similar genome
927 organization to its nearest neighbor intra-orthocluster phages (phages vB EfaS-DELF1 and IME-EFm5).
928 (C) Phage 9181 shows little to no protein homology to its nearest neighbor extra-orthocluster phages
929 (phages EFC-1 and FLA4).
930
931 **Figure S2. Phage resistant mutants of E. faecium following exposure to phages 9181, 9183 and**
932 **9184.** Phage 9181 (A), 9183 (B), and 9184 susceptibility assays and associated bacterial enumeration
933 of wild type and phage resistant mutants in the presence (white bars) or absence (black bars) of phage

934 (A-F) from three independent experiments. Phage 9181 (A, C) and phage 9183 (B, E) resistant strains
935 exhibit ≥ 5-logs of survival versus *E. faecium* Com12 and 1,141,733 (i.e. 733), respectively. Phage
936 9184 resistant strains exhibit a weak resistance phenotypes. The dotted line indicates the spontaneous
937 mutation threshold conferring phage resistance observed in the respective wild type host strain of each
938 phage.
939
940 **Figure S3. SagA is conserved in *E. faecium* Com12 and Com15.** Displayed is the BLASTP
941 alignment of SagA between Com12 and Com15, showing 95% similarity and strict conservation of
942 peptidoglycan clamp (orange lettering) and active site residues (red lettering). Colored highlights
943 indicate the location of amino acid changes detected in phage 9181 resistant mutants (81R3 and 81R4
944 – green highlight, 81R5 – yellow highlight, 81R6 – blue highlight, 81R8 – magenta highlight). Specific
945 amino acid changes are noted below the alignment in parentheses next to their respective phage
946 resistant mutant.
947
948 **Figure S4. Complementation restores phage susceptibility in phage resistant mutants.**
949 Bacterial enumeration from Phage 9181 (A and B), 9184 (C), and 9183 (D) phage susceptibility assays
950 of wild type and phage resistant mutants complemented with their respective wild type allele or empty
951 vector. Assays were performed in the presence (white bars) or absence (black bars) of phages from
952 two independent experiments. The bars and error bars indicate the average and standard deviation
953 from two independent experiments. The dotted line indicates the spontaneous mutation threshold
954 conferring phage resistance observed in the respective wild type host strain of each phage.

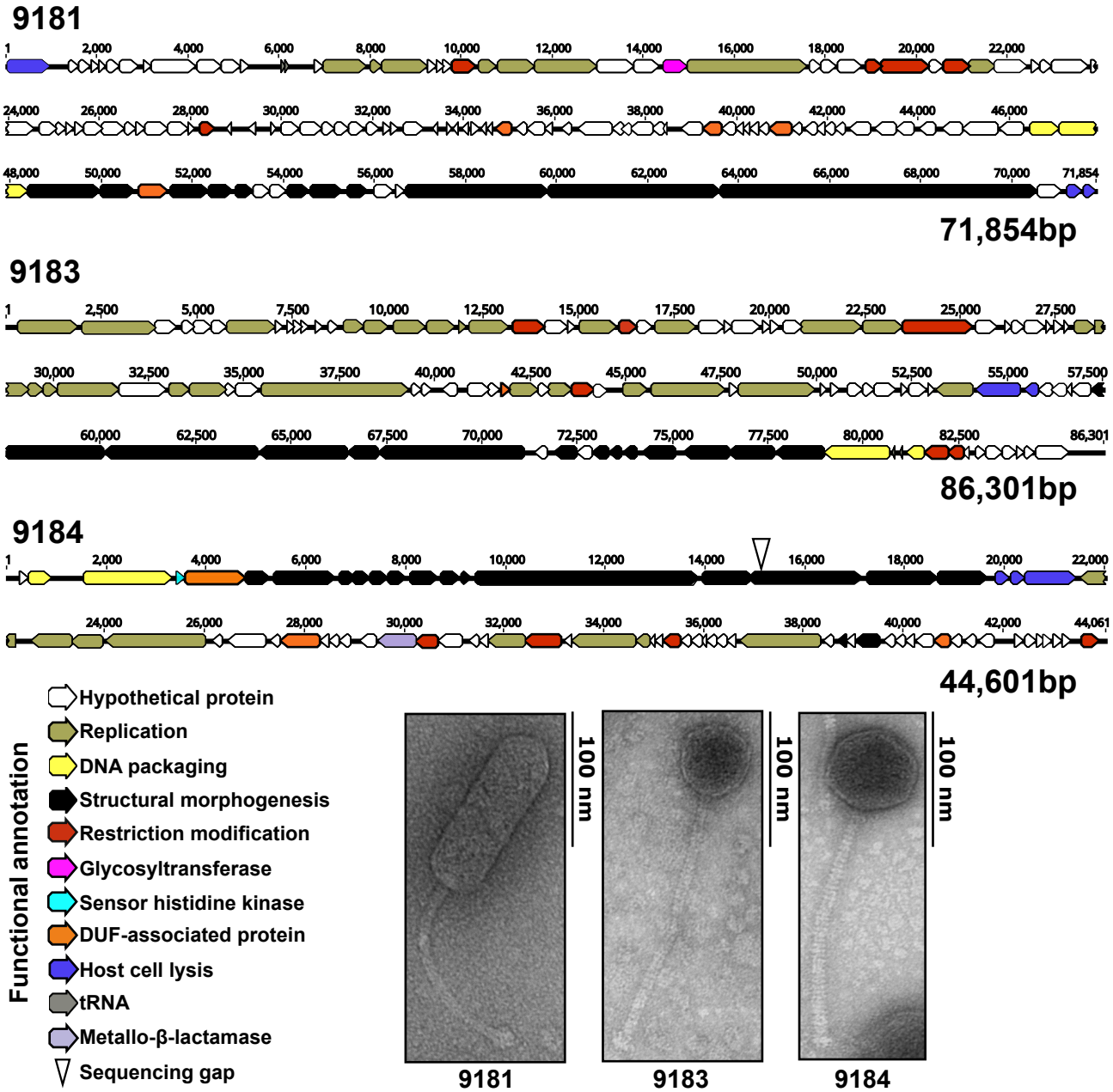
9181
71,854bp
9183
86,301bp
9184
44,601bp
Functional annotation
Hypothetical protein
Replication
DNA packaging
Structural morphogenesis
Restriction modification
Glycosyltransferase
Sensor histidine kinase
DUF-associated protein
Host cell lysis
tRNA
Metallo-β-lactamase
Sequencing gap
100 nm
100 nm
100 nm
9181
9183
9184

Figure 1

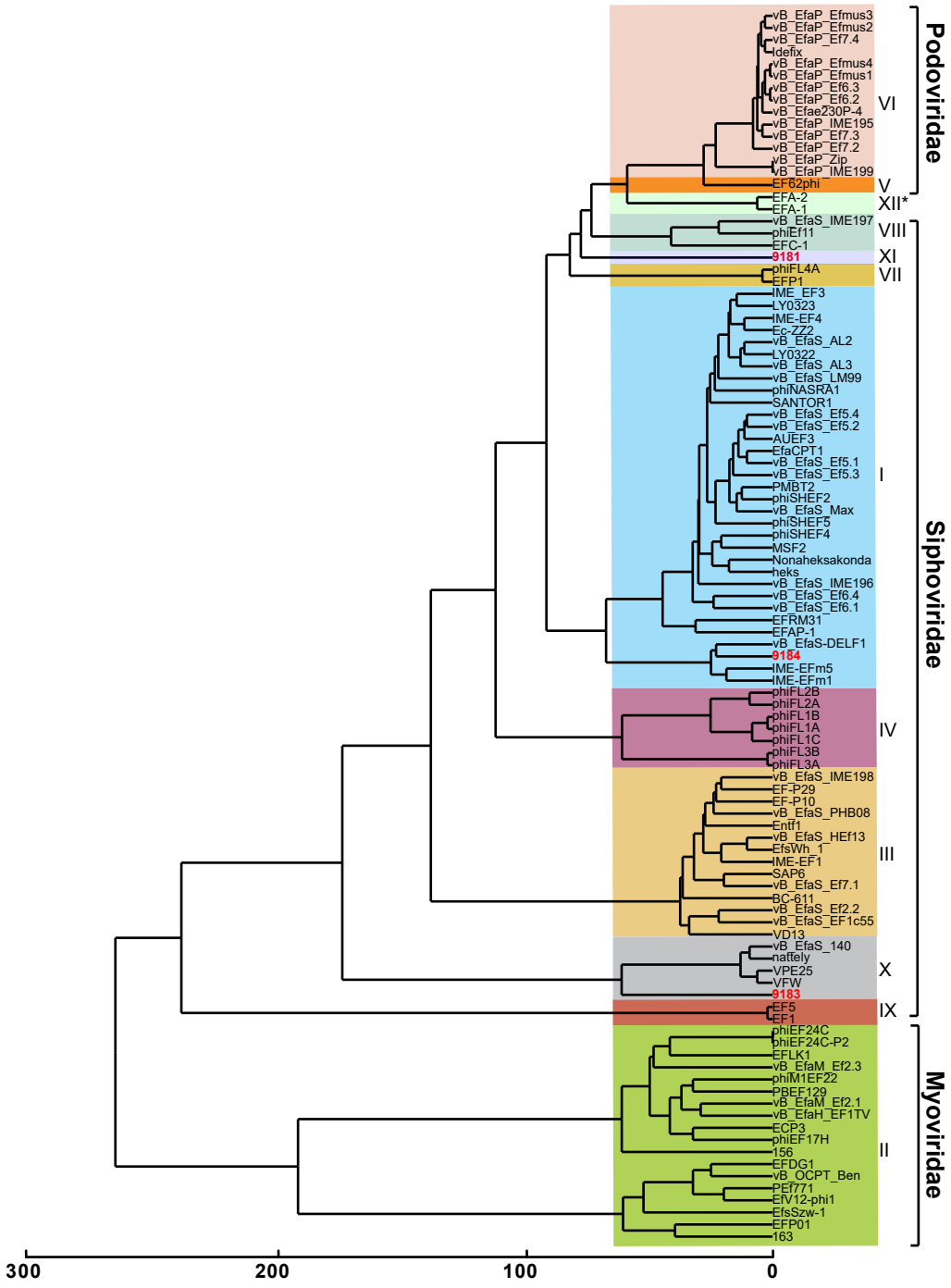
vB_EfaP_Efmus3
vB_EfaP_Efmus2
vB_EfaP_Ef7.4
Idefix
vB_EfaP_Efmus4
vB_EfaP_Efmus1
vB_EfaP_Ef6.3
vB_EfaP_Ef6.2
vB_Efae230P-4
vB_EfaP_IME195
vB_EfaP_Ef7.3
vB_EfaP_Ef7.2
vB_EfaP_Zip
vB_EfaP_IME199
EF62phi
EFA-2
EFA-1
vB_EfaS_IME197
phiEf11
EFC-1
9181
phiFL4A
EFP1
IME_EF3
LY0323
IME-EF4
Ec-ZZ2
vB_EfaS_AL2
LY0322
vB_EfaS_AL3
vB_EfaS_LM99
phiNASRA1
SANTOR1
vB_EfaS_Ef5.4
vB_EfaS_Ef5.2
AUEF3
EfaCPT1
vB_EfaS_Ef5.1
vB_EfaS_Ef5.3
PMBT2
phiSHEF2
vB_EfaS_Max
phiSHEF5
phiSHEF4
MSF2
Nonaheksakonda
heks
vB_EfaS_IME196
vB_EfaS_Ef6.4
vB_EfaS_Ef6.1
EFRM31
EFAP-1
vB_EfaS-DELF1
9184
IME-EFm5
IME-EFm1
phiFL2B
phiFL2A
phiFL1B
phiFL1A
phiFL1C
phiFL3B
phiFL3A
vB_EfaS_IME198
EF-P29
EF-P10
vB_EfaS_PHB08
Entf1
vB_EfaS_HEf13
EfsWh_1
IME-EF1
SAP6
vB_EfaS_Ef7.1
BC-611
vB_EfaS_Ef2.2
vB_EfaS_EF1c55
VD13
vB_EfaS_140
nattely
VPE25
VFW
9183
EF5
EF1
phiEF24C
phiEF24C-P2
EFLK1
vB_EfaM_Ef2.3
phiM1EF22
PBEF129
vB_EfaM_Ef2.1
vB_EfaH_EF1TV
ECP3
phiEF17H
156
EFDG1
vB_OCPT_Ben
PEf771
EfV12-phi1
EfsSzw-1
EFP01
163
VI
V
XII*
VIII
XI
VII
I
IV
III
X
IX
II
Podoviridae
Siphoviridae
Myoviridae
300
200
100
0

Figure 2

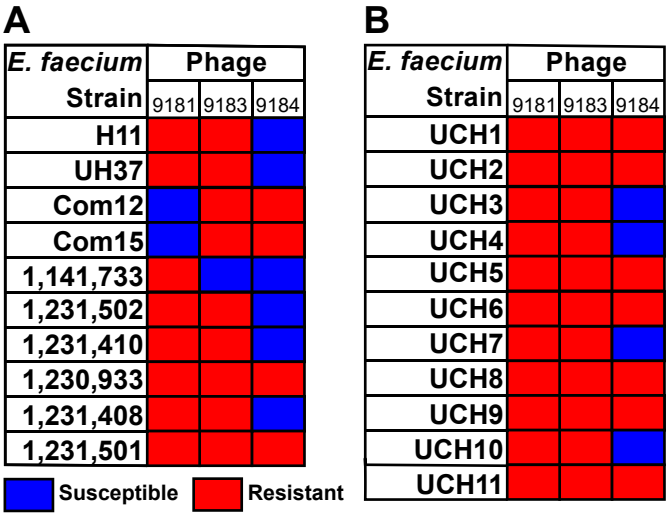
A
E. faecium Strain
Phage
9181
9183
9184
H11
UH37
Com12
Com15
1,141,733
1,231,502
1,231,410
1,230,933
1,231,408
1,231,501
Susceptible
Resistant
B
E. faecium Strain
Phage
9181
9183
9184
UCH1
UCH2
UCH3
UCH4
UCH5
UCH6
UCH7
UCH8
UCH9
UCH10
UCH11

Figure 3

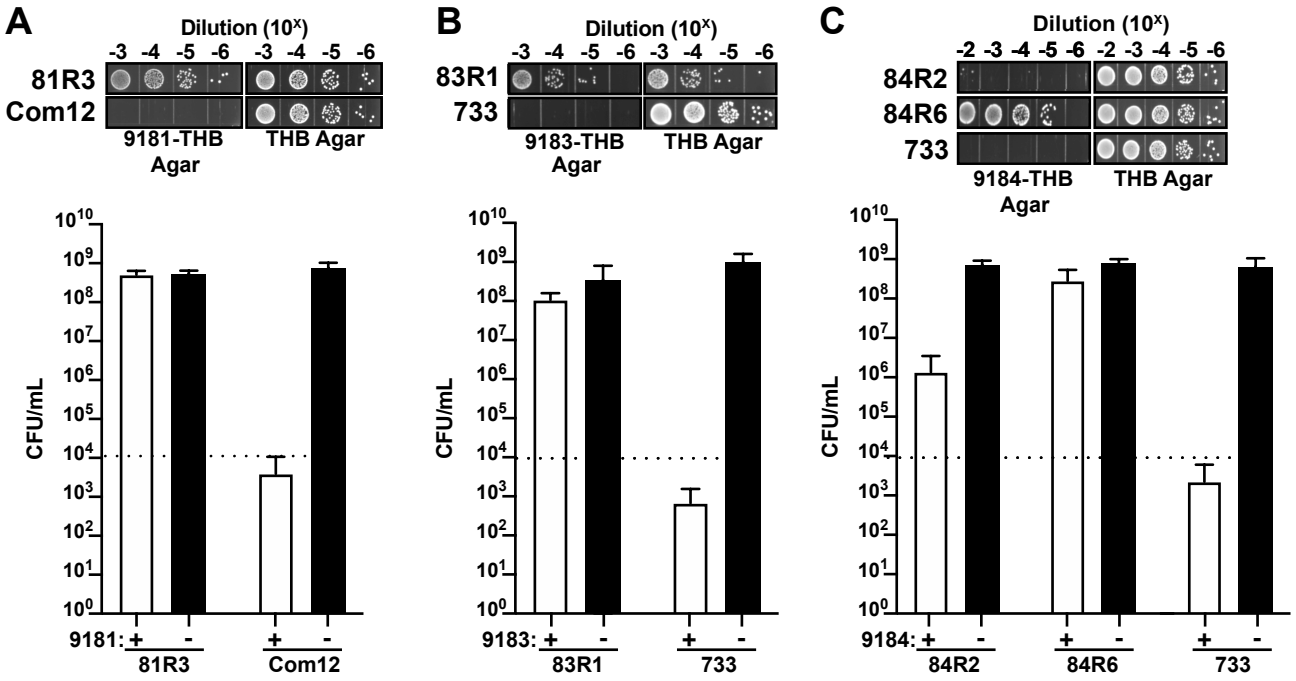
A
Dilution (10^X)
-3 -4 -5 -6 -3 -4 -5 -6
81R3
Com12
9181-THB Agar
THB Agar
CFU/mL
9181: + - + -
81R3
Com12
B
Dilution (10^X)
-3 -4 -5 -6 -3 -4 -5 -6
83R1
733
9183-THB Agar
THB Agar
CFU/mL
9183: + - + -
83R1
733
C
Dilution (10^X)
-2 -3 -4 -5 -6 -2 -3 -4 -5 -6
84R2
84R6
733
9184-THB Agar
THB Agar
CFU/mL
9184: + - + - + -
84R2
84R6
733

Figure 4

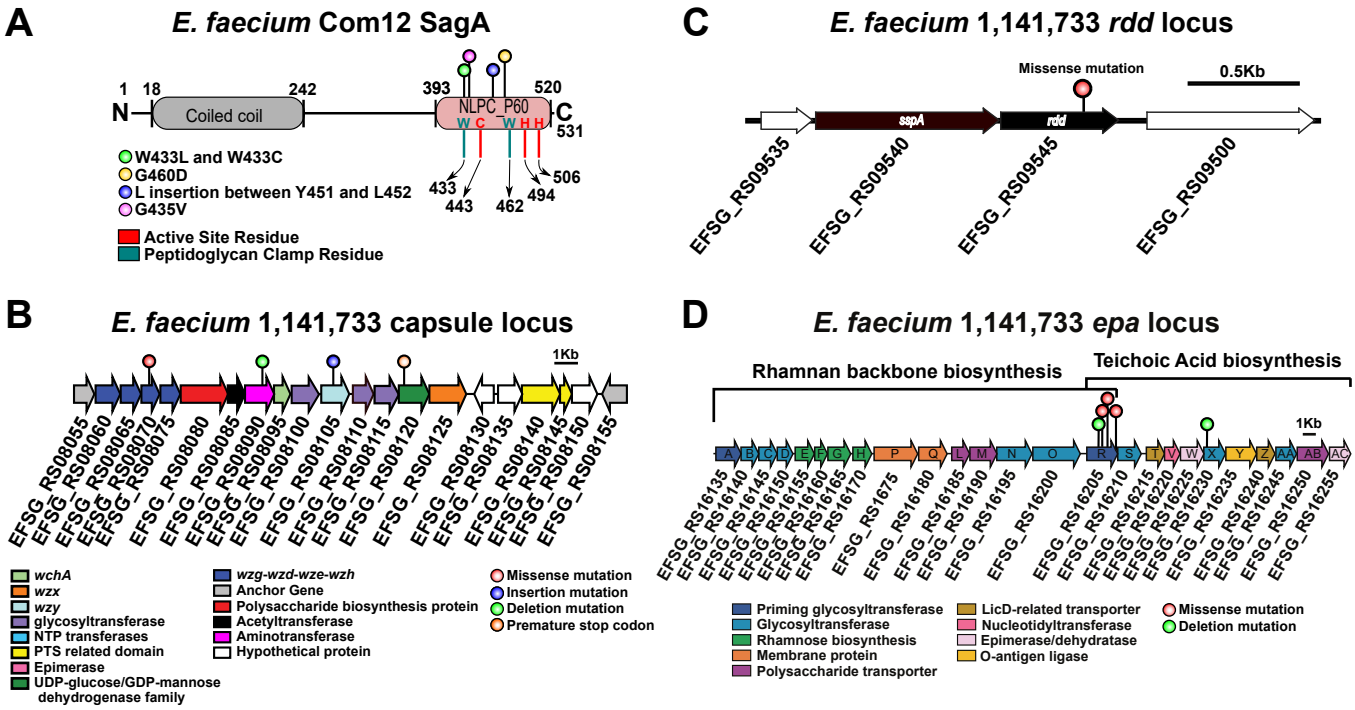
A
E. faecium Com12 SagA
1
18
242
393
520
N
Coiled coil
NLPC_P60
C
531
W C W H H
W433L and W433C
G460D
L insertion between Y451 and L452
G435V
433
443
462
494
506
Active Site Residue
Peptidoglycan Clamp Residue
B
E. faecium 1,141,733 capsule locus
1Kb
EFSG_RS08055
EFSG_RS08060
EFSG_RS08065
EFSG_RS08070
EFSG_RS08075
EFSG_RS08080
EFSG_RS08085
EFSG_RS08090
EFSG_RS08095
EFSG_RS08100
EFSG_RS08105
EFSG_RS08110
EFSG_RS08115
EFSG_RS08120
EFSG_RS08125
EFSG_RS08130
EFSG_RS08135
EFSG_RS08140
EFSG_RS08145
EFSG_RS08150
EFSG_RS08155
wchA
wzx
wzy
glycosyltransferase
NTP transferases
PTS related domain
Epimerase
UDP-glucose/GDP-mannose dehydrogenase family
wzg-wzd-wze-wzh
Anchor Gene
Polysaccharide biosynthesis protein
Acetyltransferase
Aminotransferase
Hypothetical protein
Missense mutation
Insertion mutation
Deletion mutation
Premature stop codon
C
E. faecium 1,141,733 rdd locus
Missense mutation
0.5Kb
sspA
rdd
EFSG_RS09535
EFSG_RS09540
EFSG_RS09545
EFSG_RS09500
D
E. faecium 1,141,733 epa locus
Rhamnan backbone biosynthesis
Teichoic Acid biosynthesis
1Kb
A B C D E F G H P Q L M N O R S T V W X Y Z AA AB AC
EFSG_RS16135
EFSG_RS16140
EFSG_RS16145
EFSG_RS16150
EFSG_RS16155
EFSG_RS16160
EFSG_RS16165
EFSG_RS16170
EFSG_RS1675
EFSG_RS16180
EFSG_RS16185
EFSG_RS16190
EFSG_RS16195
EFSG_RS16200
EFSG_RS16205
EFSG_RS16210
EFSG_RS16215
EFSG_RS16220
EFSG_RS16225
EFSG_RS16230
EFSG_RS16235
EFSG_RS16240
EFSG_RS16245
EFSG_RS16250
EFSG_RS16255
Priming glycosyltransferase
Glycosyltransferase
Rhamnose biosynthesis
Membrane protein
Polysaccharide transporter
LicD-related transporter
Nucleotidyltransferase
Epimerase/dehydratase
O-antigen ligase
Missense mutation
Deletion mutation

Figure 5

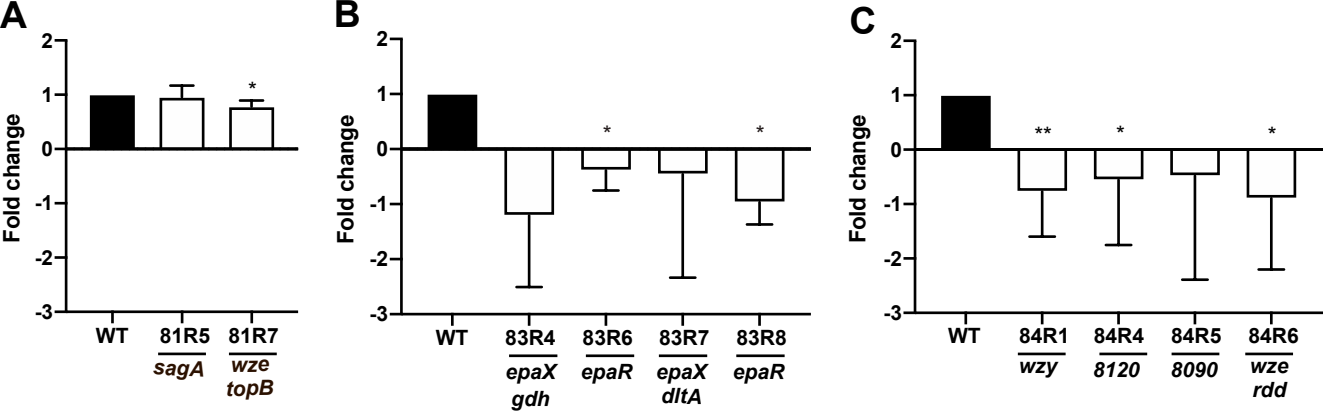
A
B
C
Fold change
2
1
0
-1
-2
-3
*
**
WT
81R5
81R7
sagA
wze
topB
83R4
83R6
83R7
83R8
epaX
gdh
epaR
epaX
dltA
epaR
84R1
84R4
84R5
84R6
wzy
8120
8090
wze
rdd

Figure 6

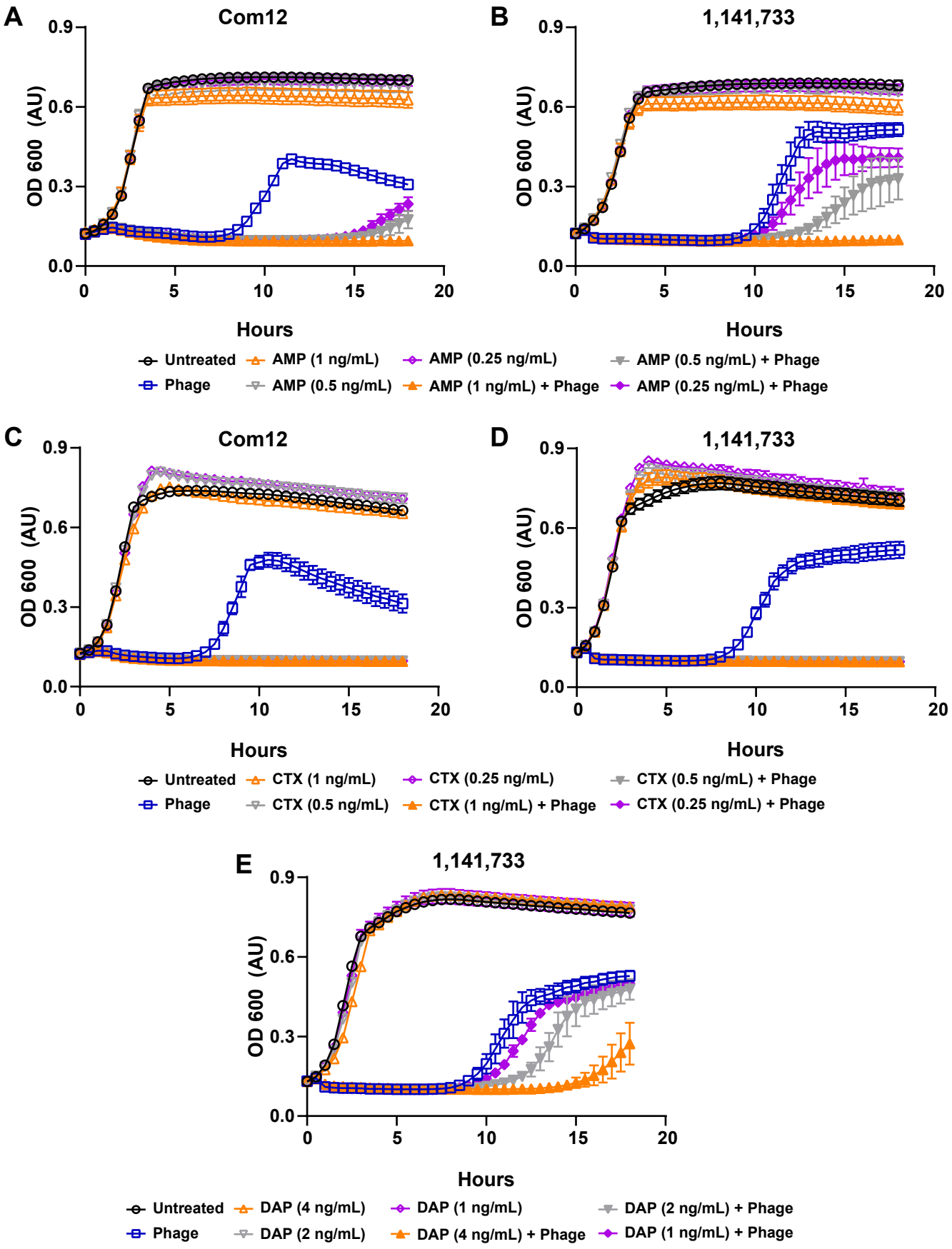
A
Com12
B
1,141,733
OD 600 (AU)
Hours
Untreated
Phage
AMP (1 ng/mL)
AMP (0.5 ng/mL)
AMP (0.25 ng/mL)
AMP (1 ng/mL) + Phage
AMP (0.5 ng/mL) + Phage
AMP (0.25 ng/mL) + Phage
C
Com12
D
1,141,733
CTX (1 ng/mL)
CTX (0.5 ng/mL)
CTX (0.25 ng/mL)
CTX (1 ng/mL) + Phage
CTX (0.5 ng/mL) + Phage
CTX (0.25 ng/mL) + Phage
E
1,141,733
DAP (4 ng/mL)
DAP (2 ng/mL)
DAP (1 ng/mL)
DAP (4 ng/mL) + Phage
DAP (2 ng/mL) + Phage
DAP (1 ng/mL) + Phage

Figure 7

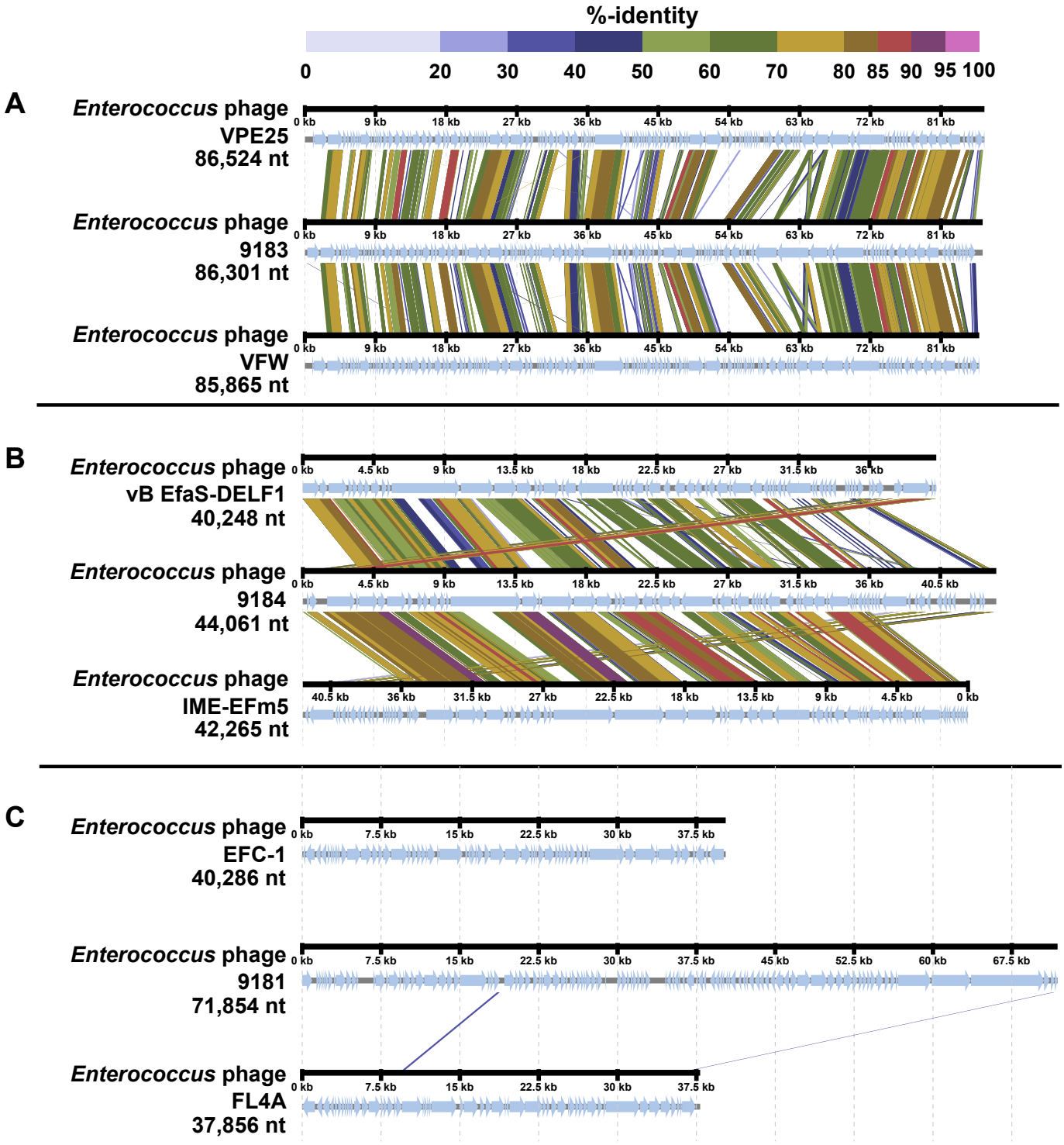
%-identity
0
20
30
40
50
60
70
80
85
90
95
100
A
Enterococcus phage VPE25 86,524 nt
Enterococcus phage 9183 86,301 nt
Enterococcus phage VFW 85,865 nt
B
Enterococcus phage vB EfaS-DELF1 40,248 nt
Enterococcus phage 9184 44,061 nt
Enterococcus phage IME-EFm5 42,265 nt
C
Enterococcus phage EFC-1 40,286 nt
Enterococcus phage 9181 71,854 nt
Enterococcus phage FL4A 37,856 nt

Figure S1

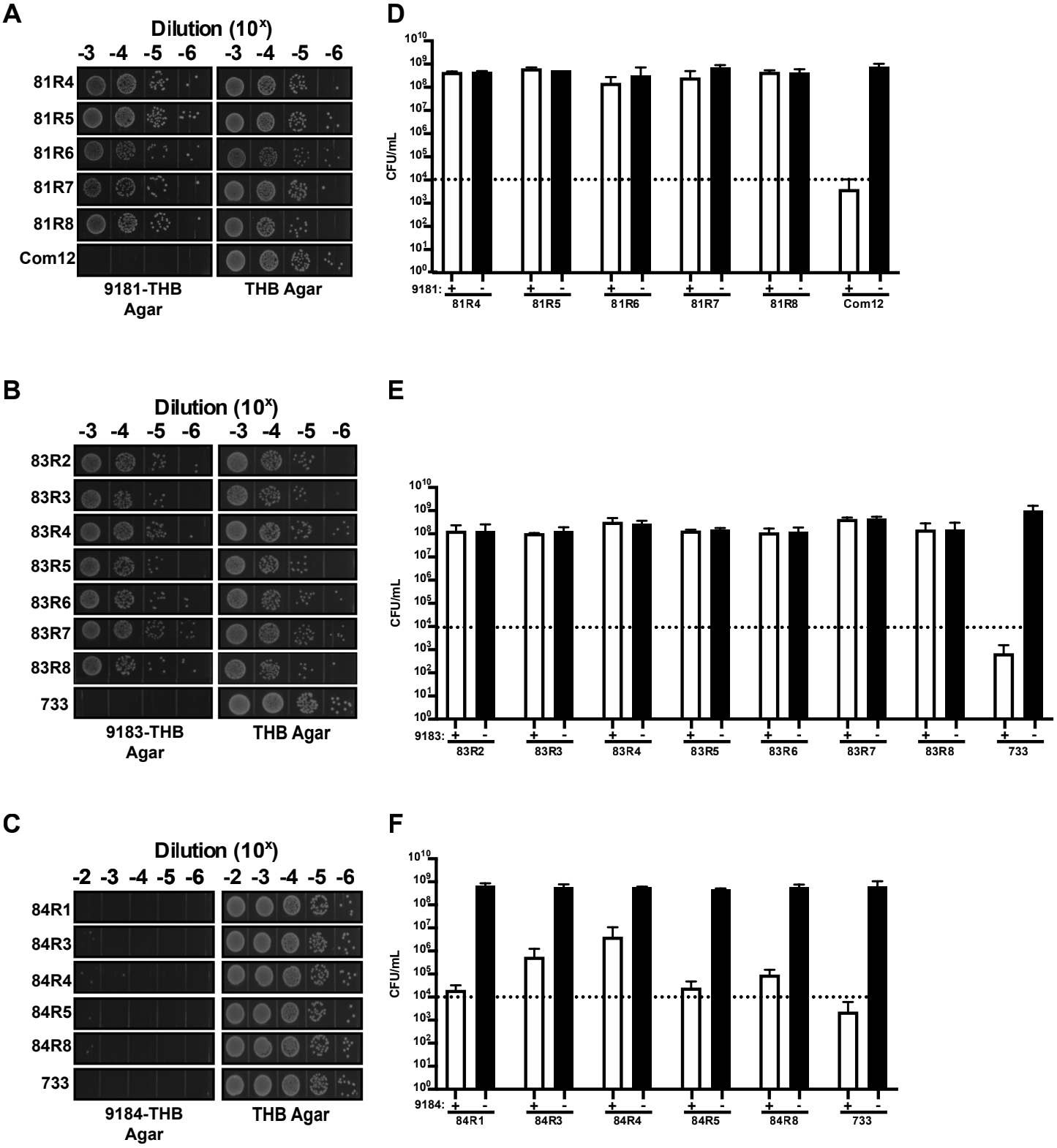
A
Dilution (10^x)
-3 -4 -5 -6 -3 -4 -5 -6
81R4
81R5
81R6
81R7
81R8
Com12
9181-THB Agar
THB Agar
B
Dilution (10^x)
-3 -4 -5 -6 -3 -4 -5 -6
83R2
83R3
83R4
83R5
83R6
83R7
83R8
733
9183-THB Agar
THB Agar
C
Dilution (10^x)
-2 -3 -4 -5 -6 -2 -3 -4 -5 -6
84R1
84R3
84R4
84R5
84R8
733
9184-THB Agar
THB Agar
D
CFU/mL
9181:
81R4
81R5
81R6
81R7
81R8
Com12
E
CFU/mL
9183:
83R2
83R3
83R4
83R5
83R6
83R7
83R8
733
F
CFU/mL
9184:
84R1
84R3
84R4
84R5
84R8
733

Figure S2

Identities	Positives	Gaps
513/538(95%)	515/538(95%)	20/538(3%)

```
Com12  1    VKKSLISAVMVCSMTLTAVASPIAAAADDFDSQIQQQDQKIADLKNQQADAQSQIDALES  60
            +KKSLISAVMVCSMTLTAVASPIAAAADDFDSQIQQQDQKIADLKNQQADAQSQIDALES
Com15  1    MKKSLISAVMVCSMTLTAVASPIAAAADDFDSQIQQQDQKIADLKNQQADAQSQIDALES  60

Com12  61   QVSEINTQAQDLLAKQDTLRQESAQLVKDIADLQERIEKREDTIQKQAREAQVSNTSSNY  120
            QVSEINTQAQDLLAKQDTLRQESAQLVKDIADLQERIEKREDTIQKQAREAQVSNTSSNY
Com15  61   QVSEINTQAQDLLAKQDTLRQESAQLVKDIADLQERIEKREDTIQKQAREAQVSNTSSNY  120

Com12  121  IDAVLNADSLADAIGRVQAMTTMVKANNDLMEQQKQDKKAVEDKKAENDAKLKELAENQA  180
            IDAVLNADSLADAIGRVQAMTTMVKANNDLMEQQKQDKKAVEDKKAENDAKLKELAENQA
Com15  121  IDAVLNADSLADAIGRVQAMTTMVKANNDLMEQQKQDKKAVEDKKAENDAKLKELAENQA  180

Com12  181  ALESQKGDLLSKQADLNVLKTSLAAEQATAEDKKADLNRQKAEAEAEQARIREQQRLAEQ  240
            ALESQKGDLLSKQADLNVLKTSLAAEQATAEDKKADLNRQKAEAEAEQARIREQQRLAEQ
Com15  181  ALESQKGDLLSKQADLNVLKTSLAAEQATAEDKKADLNRQKAEAEAEQARIREQQRLAEQ  240

Com12  241  ARQQAAQEKAEKEAREQAEAEAQATQASSTAQSSASEESSAAQSSTTEESSSAAQSSTTE  300
            ARQQAAQEKAEKEAREQAEAEAQATQASS AQSSA+EESSAAQSSTTEESSSAAQSSTTE
Com15  241  ARQQAAQEKAEKEAREQAEAEAQATQASSAAQSSATEESSAAQSSTTEESSSAAQSSTTE  300

Com12  301  ESTTAPESSTTEESTTAPESSTTEESTTVPESSTTEESTTVPESSTTEESTTVPESSTTE  360
            ESTTAPESSTTEESTT PESSTTEESTT PESSTTEESTTVPESSTTEESTTVPES
Com15  301  ESTTAPESSTTEESTTXPESSTTEESTTAPESSTTEESTTVPESSTTEESTTVPES----  356

Com12  361  ESTTVPETSTEESTTPAPTTPSTDQSVDPGNSTGSNATNNT--------TNTTPTPTPSG  412
                    STEESTTPAPTTPSTDQSVDPGNSTGSNATNNT        TNTTPTPTPSG
Com15  357  --------STEESTTPAPTTPSTDQSVDPGNSTGSNATNNTTNTTPXXXTNTTPTPTPSG  408

Com12  413  SVNGAAIVAEAYKYIGTPYVWGGKDPSGFDCSGFTRYVYLQVTGRDIGGWTVPQESAGTK  472
            SVNGAAIVAEAYKYIGTPYVWGGKDPSGFDCSGFTRYVYLQVTGRDIGGWTVPQESAGTK
Com15  409  SVNGAAIVAEAYKYIGTPYVWGGKDPSGFDCSGFTRYVYLQVTGRDIGGWTVPQESAGTK  468

Com12  473  ISVSQAKAGDLLFWGSPGGTYHVAIALGGGQYIHAPQPGESVKVGSVQWFAPDFAVSM  530
            ISVSQAKAGDLLFWGSPGGTYHVAIALGGGQYIHAPQPGESVKVGSVQWFAPDFAVSM
Com15  469  ISVSQAKAGDLLFWGSPGGTYHVAIALGGGQYIHAPQPGESVKVGSVQWFAPDFAVSM  526
```

81R3 and 81R4 (W433G and W433C, respectively)
81R5 (G460D)
81R6 (note: L insertion between Y451 and L452
81R8 (G435V)
Active Site Residues (C443, H494, H506)
Peptidoglycan Clamp Residues (W433 and W462)

Figure S3

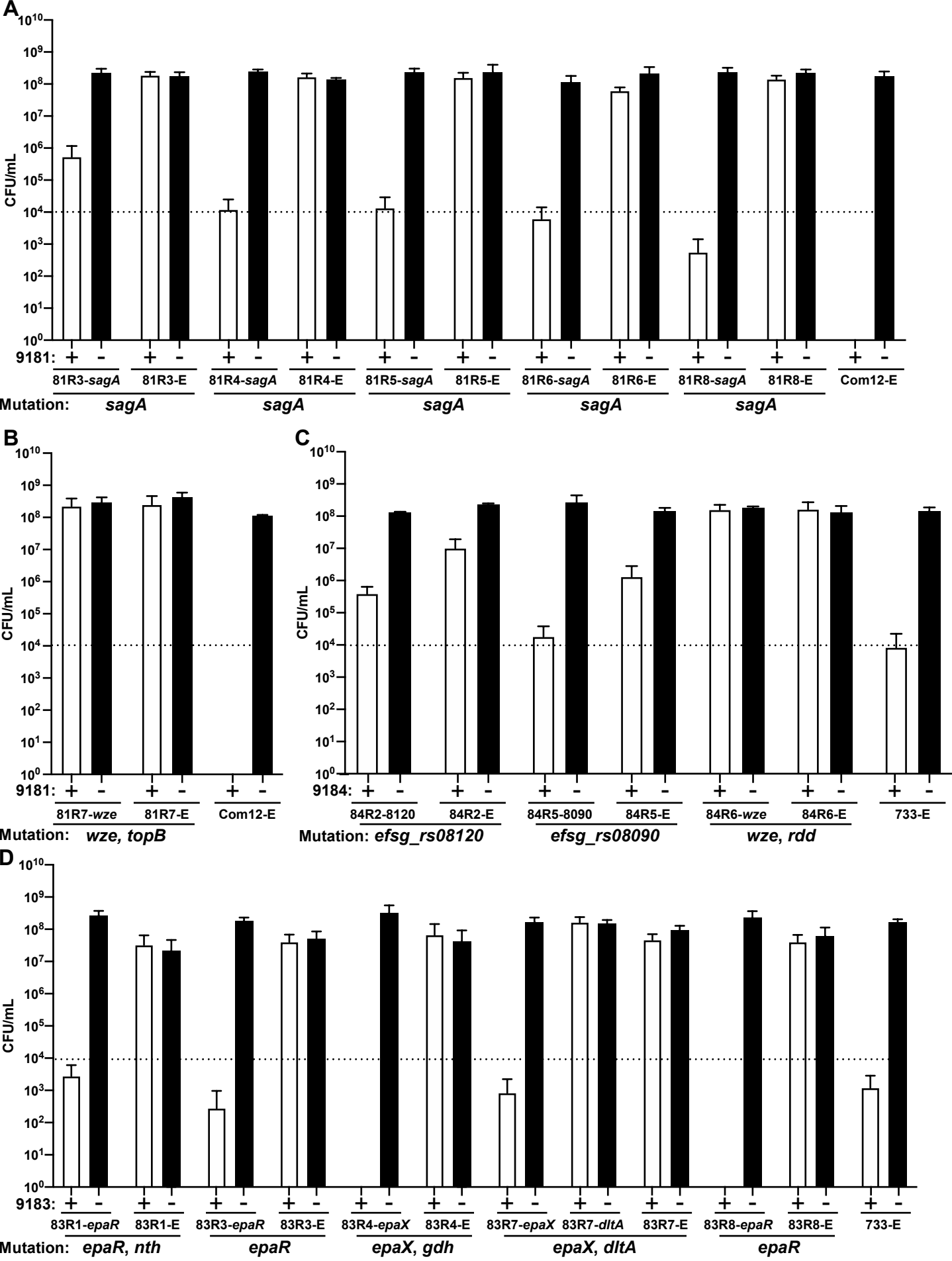
A
CFU/mL
9181:
81R3-sagA
81R3-E
81R4-sagA
81R4-E
81R5-sagA
81R5-E
81R6-sagA
81R6-E
81R8-sagA
81R8-E
Com12-E
Mutation: sagA
B
9181:
81R7-wze
81R7-E
Com12-E
Mutation: wze, topB
C
9184:
84R2-8120
84R2-E
84R5-8090
84R5-E
84R6-wze
84R6-E
733-E
Mutation: efsg_rs08120
efsg_rs08090
wze, rdd
D
9183:
83R1-epaR
83R1-E
83R3-epaR
83R3-E
83R4-epaX
83R4-E
83R7-epaX
83R7-dltA
83R7-E
83R8-epaR
83R8-E
733-E
Mutation: epaR, nth
epaR
epaX, gdh
epaX, dltA
epaR

Figure S4